Density Model for Beaked Whales (*Mesoplodon spp. and Ziphius cavirostris*) for the U.S. Gulf of Mexico: Supplementary Report

Duke University Marine Geospatial Ecology Lab*

Model Version 1.4 - 2016-03-09

Citation

When referencing our methodology or results generally, please cite our open-access article:

Roberts JJ, Best BD, Mannocci L, Fujioka E, Halpin PN, Palka DL, Garrison LP, Mullin KD, Cole TVN, Khan CB, McLellan WM, Pabst DA, Lockhart GG (2016) Habitat-based cetacean density models for the U.S. Atlantic and Gulf of Mexico. Scientific Reports 6: 22615. doi: 10.1038/srep22615

To reference this specific model or Supplementary Report, please cite:

Roberts JJ, Best BD, Mannocci L, Fujioka E, Halpin PN, Palka DL, Garrison LP, Mullin KD, Cole TVN, Khan CB, McLellan WM, Pabst DA, Lockhart GG (2016) Density Model for Beaked Whales (*Mesoplodon spp. and Ziphius cavirostris*) for the U.S. Gulf of Mexico Version 1.4, 2016-03-09, and Supplementary Report. Marine Geospatial Ecology Lab, Duke University, Durham, North Carolina.

Copyright and License

Revision History

Version	Date	Description of changes
1	2014-10-20	Initial version.
1.1	2015-02-02	Updated the documentation. No changes to the model.
1.2	2015-05-14	Updated calculation of CVs. Switched density rasters to logarithmic breaks. No changes to the model.
1.3	2015-09-29	Updated the documentation. No changes to the model.
1.4	2016-03-09	Changed document title to clarify that Ziphius cavirostris is included in this model. No changes to the model or other parts of the documentation.

*For questions, or to offer feedback about this model or report, please contact Jason Roberts (jason.roberts@duke.edu)

Survey Data

Survey	Period	Length (1000 km)	Hours	Sightings
SEFSC GOMEX92-96 Aerial Surveys	1992-1996	27	152	0
SEFSC Gulf of Mexico Shipboard Surveys, 2003-2009	2003-2009	19	1156	27
SEFSC GulfCet I Aerial Surveys	1992-1994	50	257	12
SEFSC GulfCet II Aerial Surveys	1996-1998	22	124	7
SEFSC GulfSCAT 2007 Aerial Surveys	2007-2007	18	95	0
SEFSC Oceanic CetShip Surveys	1992-2001	49	3102	66
SEFSC Shelf CetShip Surveys	1994-2001	10	707	4
Total		195	5593	116

Table 2: Survey effort and sightings used in this model. Effort is tallied as the cumulative length of on-effort transects and hours the survey team was on effort. Sightings are the number of on-effort encounters of the modeled species for which a perpendicular sighting distance (PSD) was available. Off effort sightings and those without PSDs were omitted from the analysis.

Period	Length (1000 km)	Hours	Sightings
1992-2009	195	5592	116
1998-2009	62	2679	46
% Lost	68	52	60

Table 3: Survey effort and on-effort sightings having perpendicular sighting distances. % Lost shows the percentage of effort or sightings lost by restricting the analysis to surveys performed in 1998 and later, the era in which remotely-sensed chlorophyll and derived productivity estimates are available. See Figure 1 for more information.

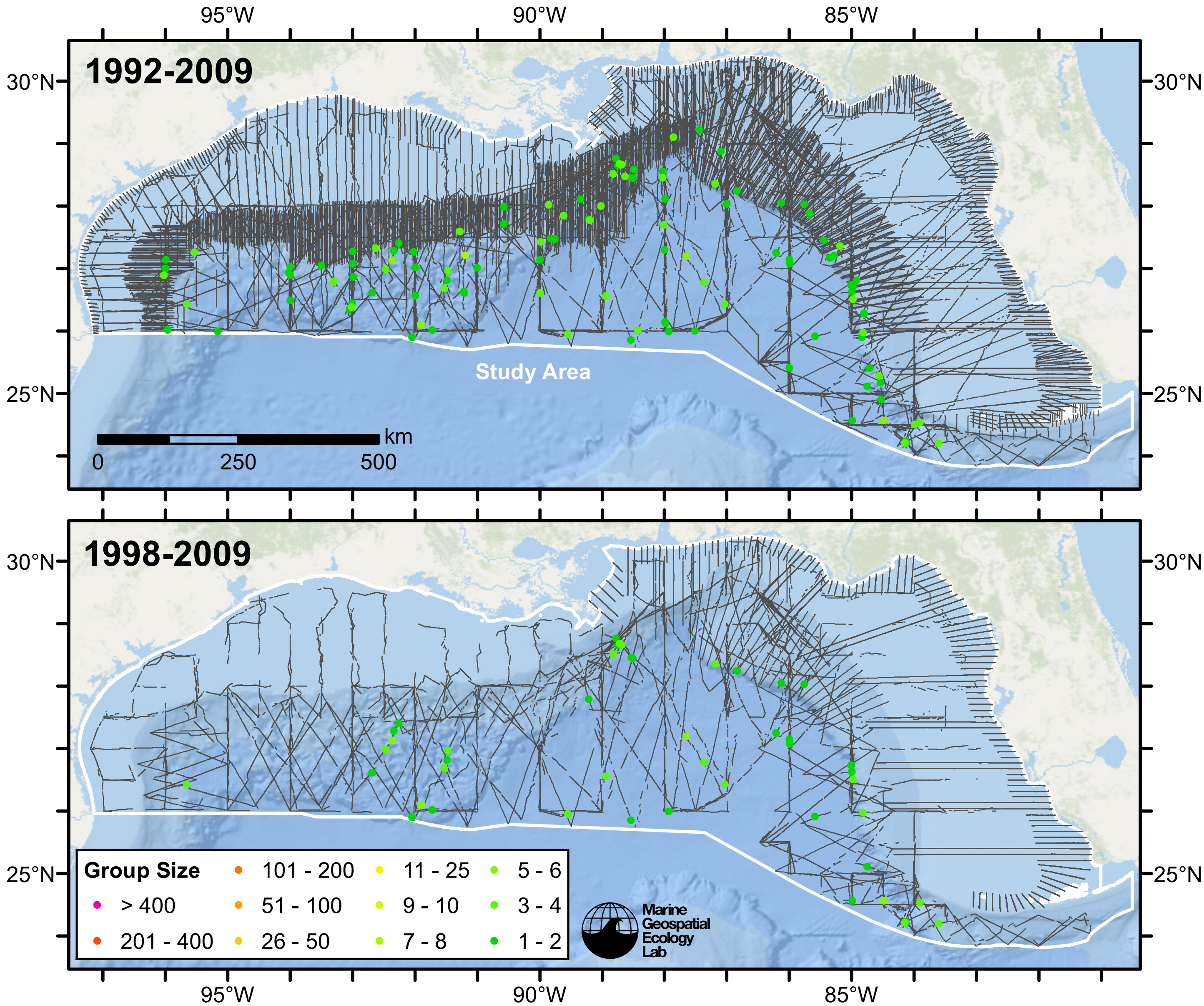

Figure 1: Beaked whales sightings and survey tracklines. The top map shows all surveys. The bottom map shows surveys performed in 1998 or later. the era in which remotely-sensed chlorophyll and derived productivity estimates are available. Models fitted to contemporaneous (day-of-sighting) estimates of those predictors only utilize these surveys. These maps illustrate the survey data lost in order to utilize those predictors. Models fitted to climatogical estimates of those predictors do not suffer this data loss.

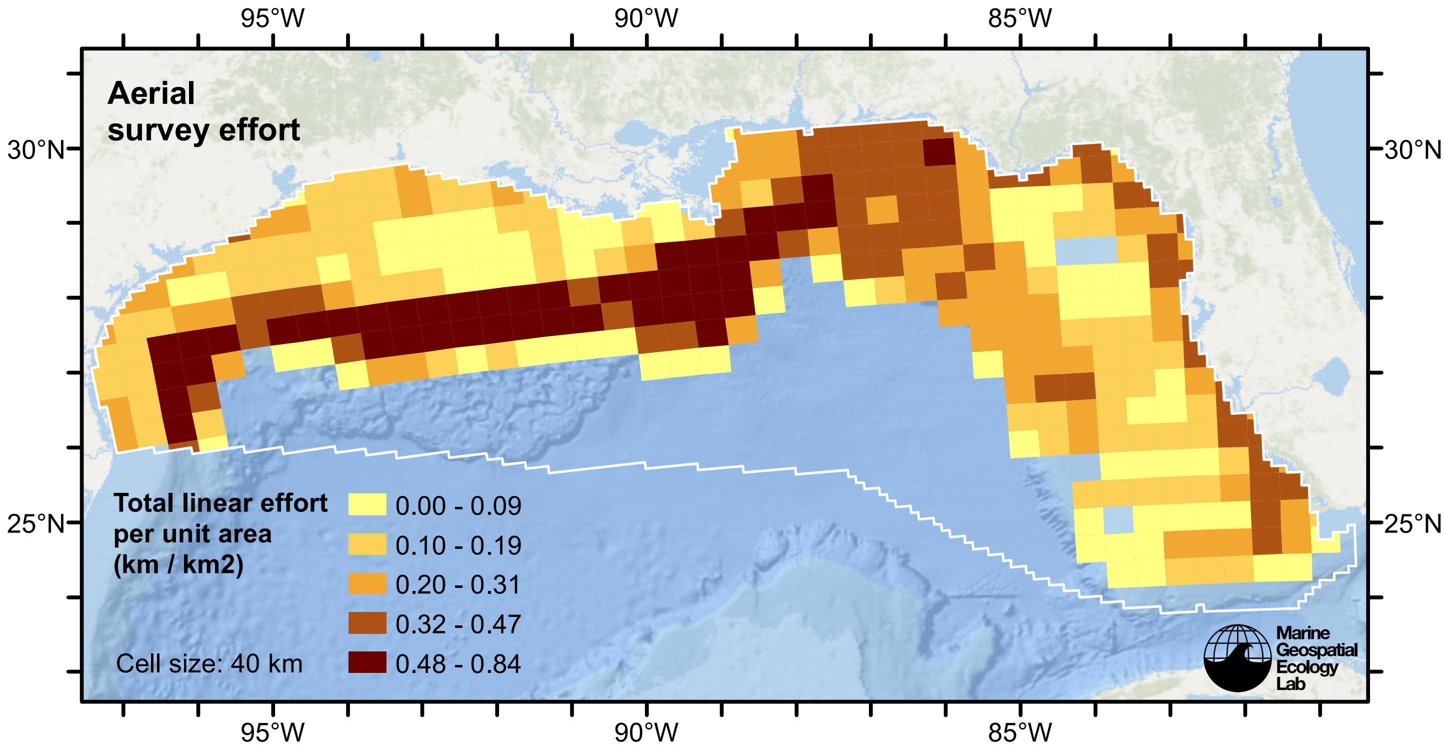

Figure 2: Aerial linear survey effort per unit area.

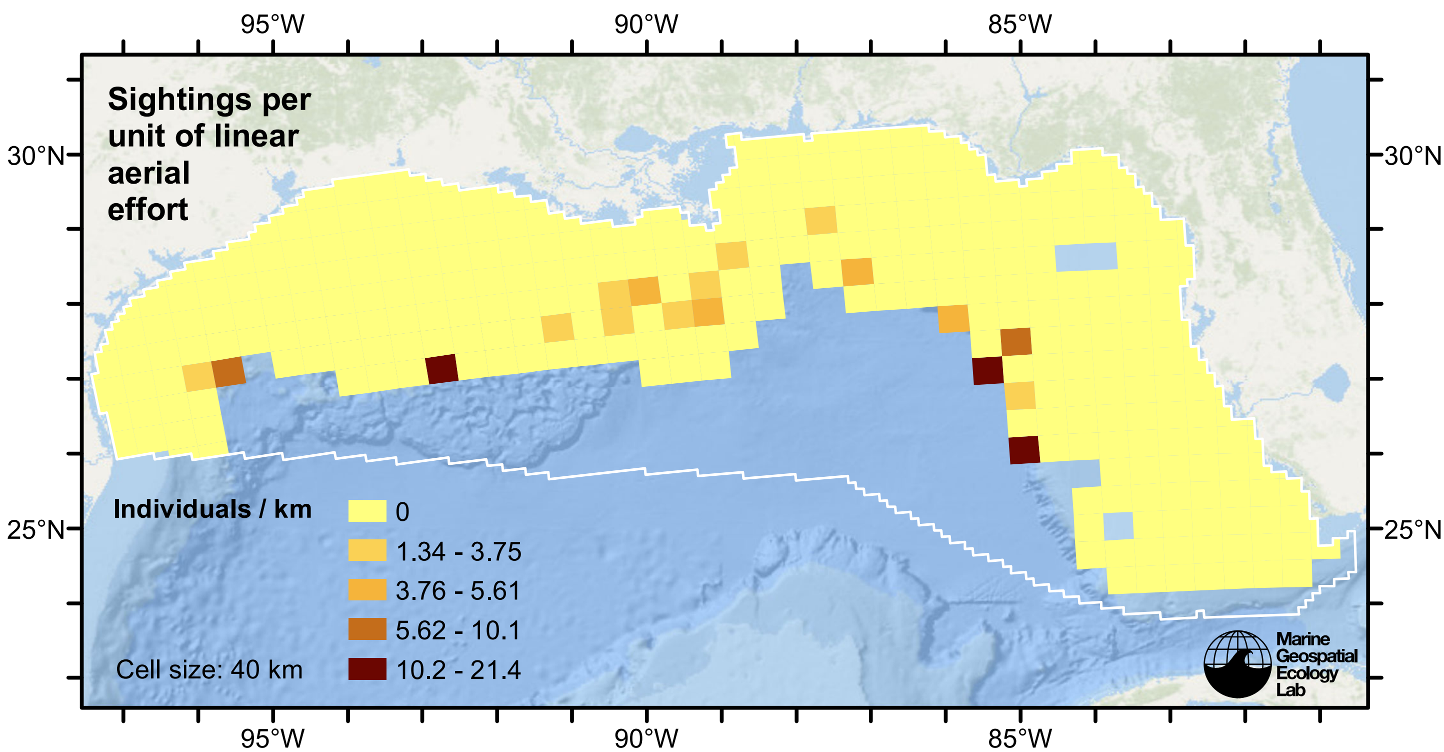

Figure 3: Beaked whales sightings per unit aerial linear survey effort.

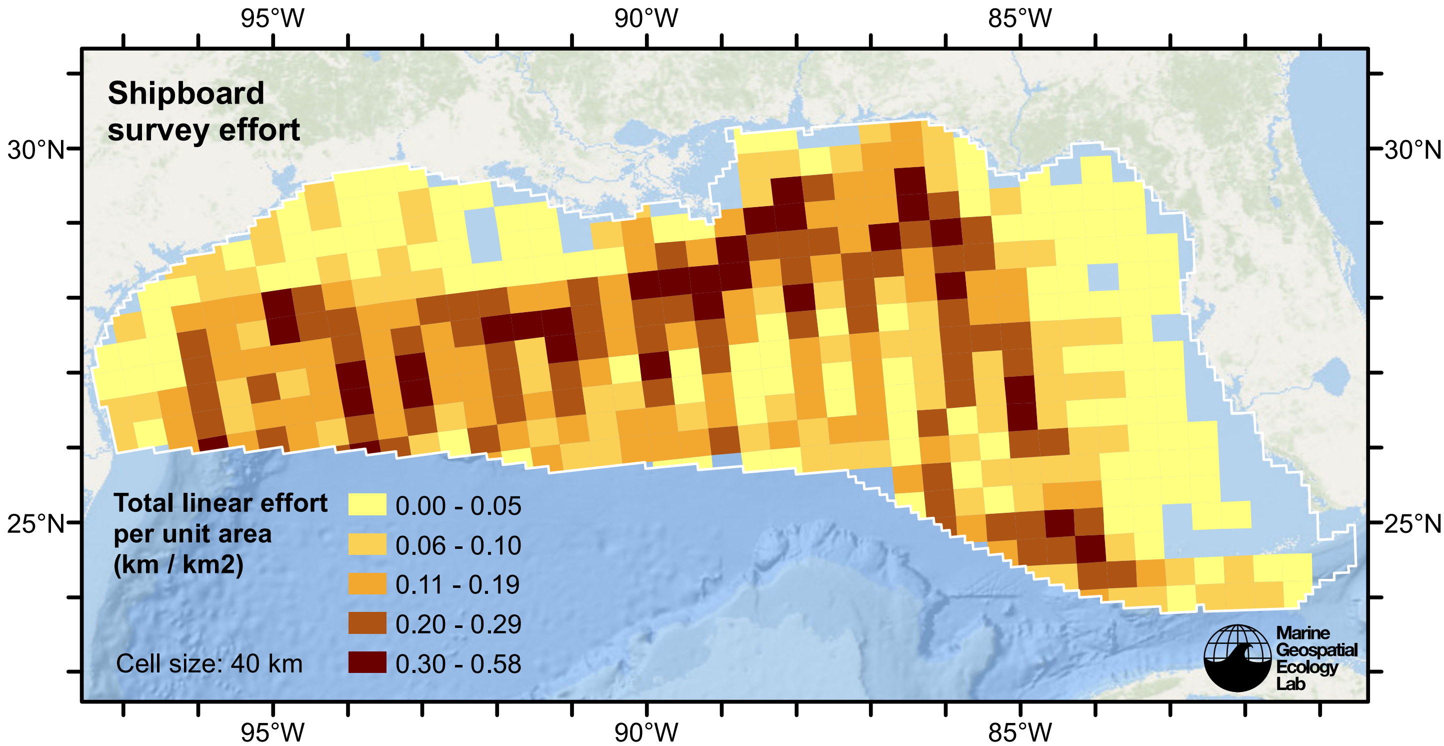

Figure 4: Shipboard linear survey effort per unit area.

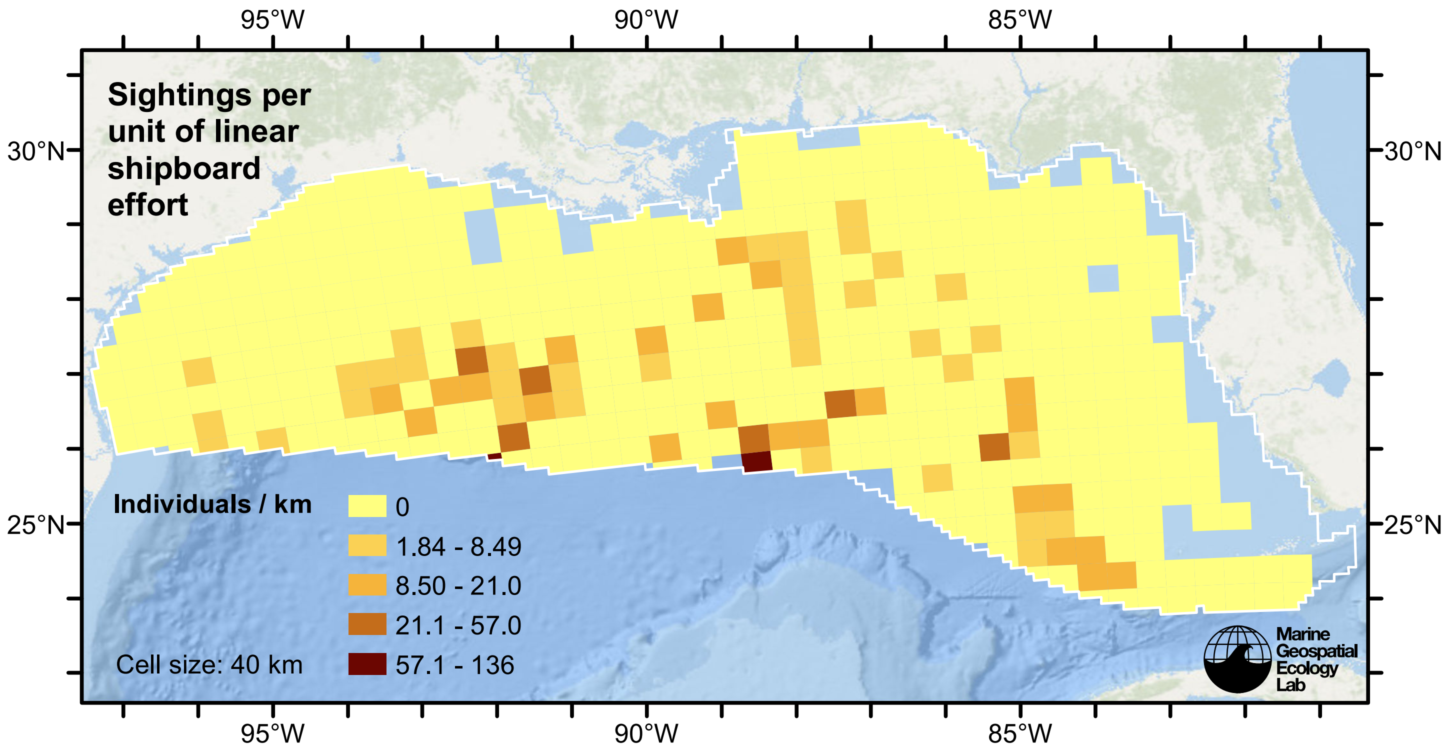

Figure 5: Beaked whales sightings per unit shipboard linear survey effort.

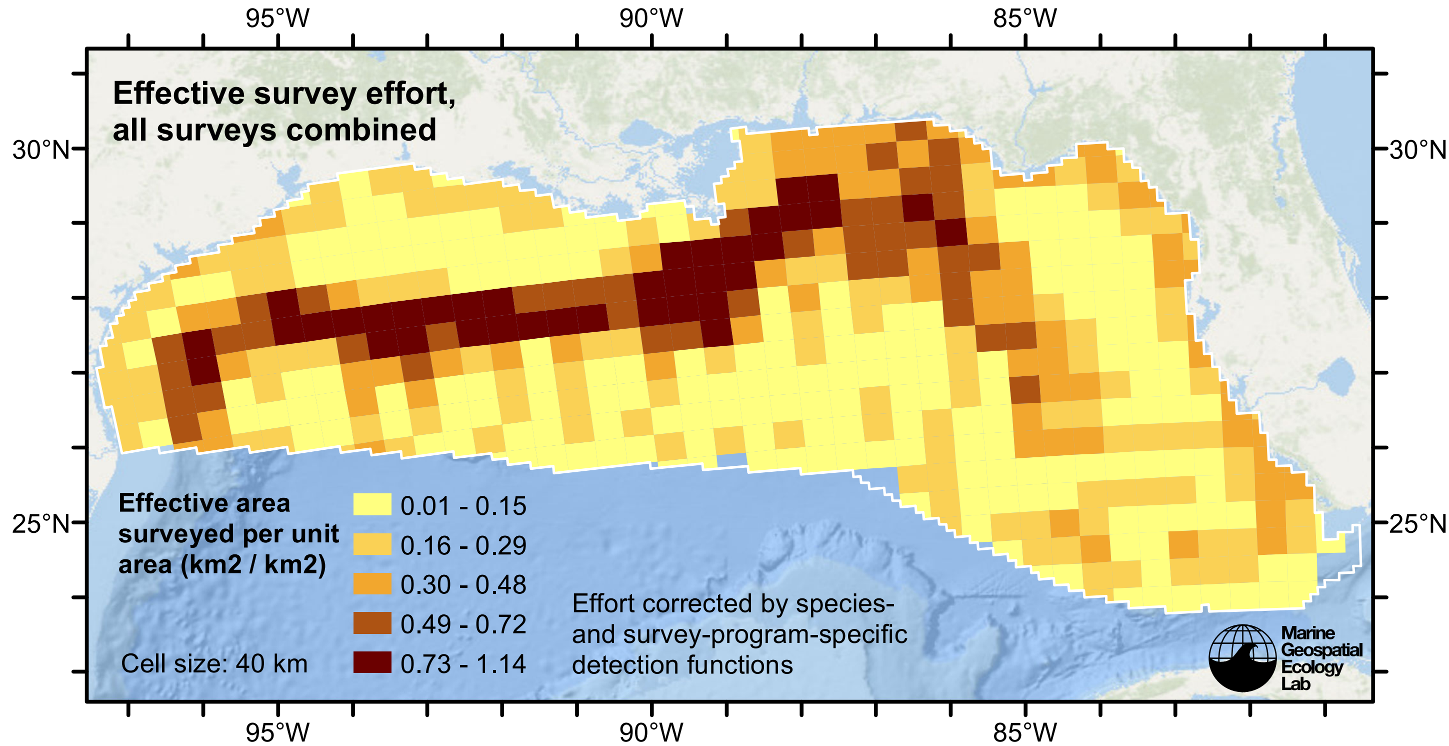

Figure 6: Effective survey effort per unit area, for all surveys combined. Here, effort is corrected by the species- and survey-program-specific detection functions used in fitting the density models.

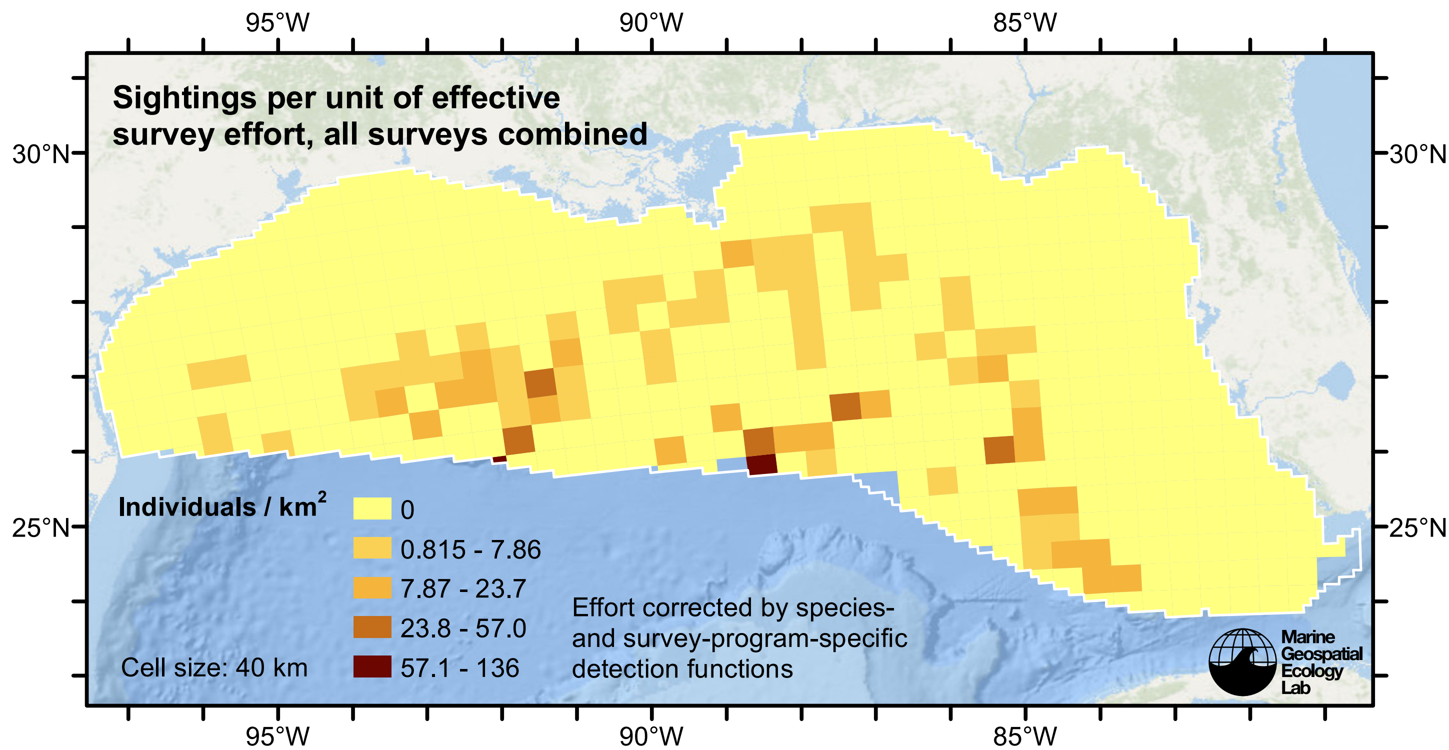

Figure 7: Beaked whales sightings per unit of effective survey effort, for all surveys combined. Here, effort is corrected by the species- and survey-program-specific detection functions used in fitting the density models.

Detection Functions

The detection hierarchy figures below show how sightings from multiple surveys were pooled to try to achieve Buckland et. al's (2001) recommendation that at least 60-80 sightings be used to fit a detection function. Leaf nodes, on the right, usually represent individual surveys, while the hierarchy to the left shows how they have been grouped according to how similar we believed the surveys were to each other in their detection performance.

At each node, the red or green number indicates the total number of sightings below that node in the hierarchy, and is colored green if 70 or more sightings were available, and red otherwise. If a grouping node has zero sightings–i.e. all of the surveys within it had zero sightings–it may be collapsed and shown as a leaf to save space.

Each histogram in the figure indicates a node where a detection function was fitted. The actual detection functions do not appear in this figure; they are presented in subsequent sections. The histogram shows the frequency of sightings by perpendicular sighting distance for all surveys contained by that node. Each survey (leaf node) recieves the detection function that is closest to it up the hierarchy. Thus, for common species, sufficient sightings may be available to fit detection functions deep in the hierarchy, with each function applying to only a few surveys, thereby allowing variability in detection performance between surveys to be addressed relatively finely. For rare species, so few sightings may be available that we have to pool many surveys together to try to meet Buckland's recommendation, and fit only a few coarse detection functions high in the hierarchy.

A blue Proxy Species tag indicates that so few sightings were available that, rather than ascend higher in the hierarchy to a point that we would pool grossly-incompatible surveys together, (e.g. shipboard surveys that used big-eye binoculars with those that used only naked eyes) we pooled sightings of similar species together instead. The list of species pooled is given in following sections.

Shipboard Surveys

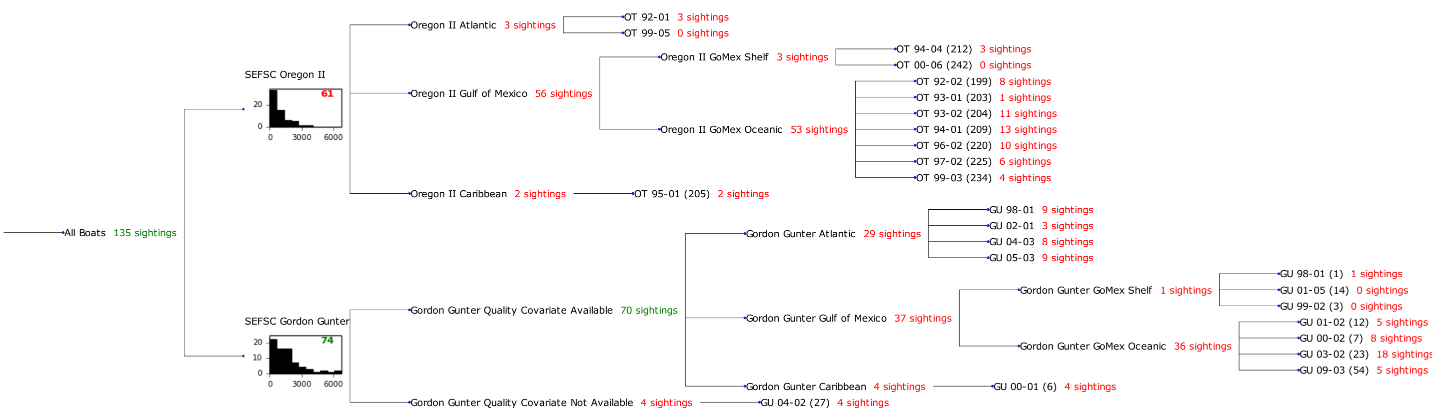

Figure 8: Detection hierarchy for shipboard surveys

SEFSC Oregon II

The sightings were right truncated at 3000m.

Covariate	Description
beaufort	Beaufort sea state.
quality	Survey-specific index of the quality of observation conditions, utilizing relevant factors other than Beaufort sea state (see methods).
size	Estimated size (number of individuals) of the sighted group.

Table 4: Covariates tested in candidate "multi-covariate distance sampling" (MCDS) detection functions.

Key	Adjustment	Order	Covariates	Succeeded	Δ AIC	Mean ESHW (m)
hn			size	Yes	0.00	1462
hn			quality, size	Yes	1.87	1464
hn			beaufort, size	Yes	1.94	1439
hn			beaufort, quality, size	Yes	3.81	1443
hr			size	Yes	4.42	1834
hr			beaufort, size	Yes	6.07	1870
hr			quality, size	Yes	6.30	1855
hr			beaufort, quality, size	Yes	7.97	1879
hn			beaufort	Yes	12.65	1399
hn			beaufort, quality	Yes	12.80	1386
hn	cos	2		Yes	13.73	1009
hr				Yes	13.84	838
hr			quality	Yes	14.86	818
hr			beaufort	Yes	14.96	1086
hr	poly	4		Yes	15.59	804
hr	poly	2		Yes	15.84	838
hr			beaufort, quality	Yes	16.30	895
hn	cos	3		Yes	16.79	1027
hn			quality	Yes	17.29	1424
hn				Yes	19.39	1390
hn	herm	4		Yes	21.25	1386

Table 5: Candidate detection functions for SEFSC Oregon II. The first one listed was selected for the density model.

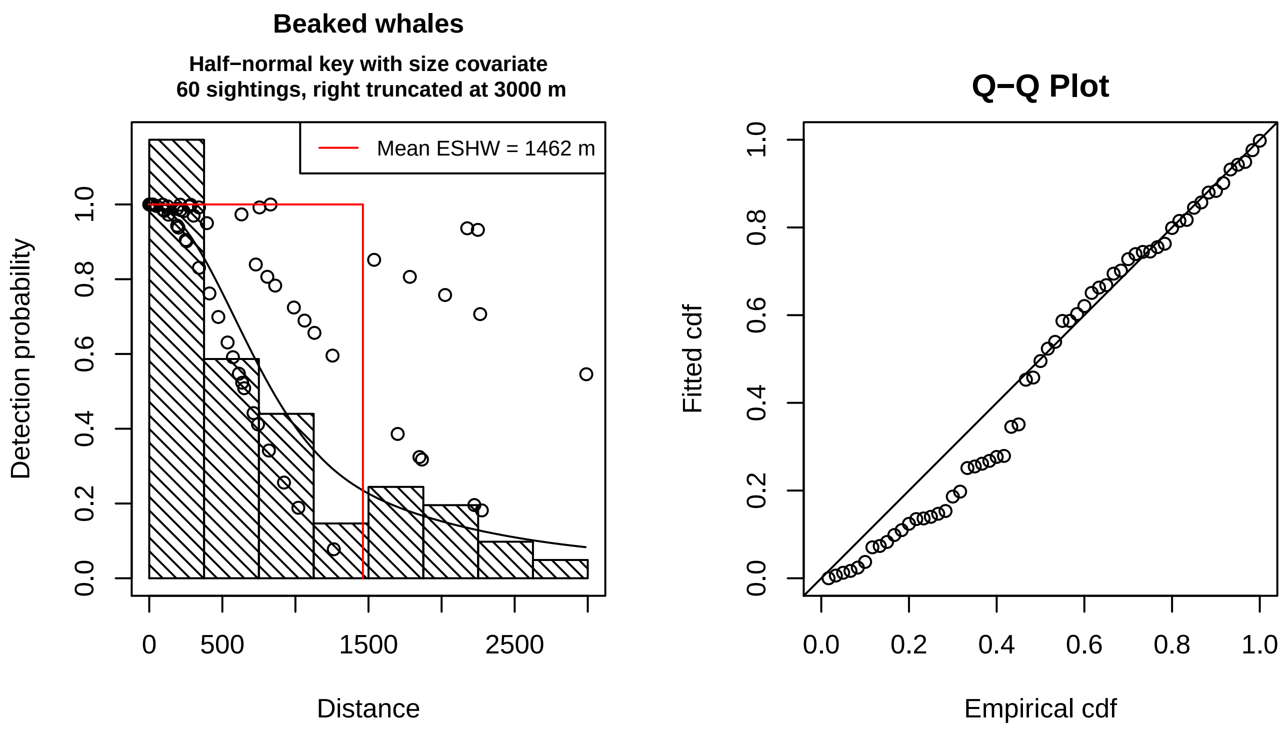

Figure 9: Detection function for SEFSC Oregon II that was selected for the density model

Statistical output for this detection function:

```
Summary for ds object
Number of observations :  60
Distance range         :  0  -  3000
AIC                    :  907.5095

Detection function:
 Half-normal key function

Detection function parameters
Scale Coefficients:
             estimate        se
(Intercept) 5.5341163 0.3555944
size        0.7910727 0.2350197

                        Estimate          SE        CV
Average p              0.3665947  0.04554777 0.1242456
N in covered region 163.6684827 27.38895820 0.1673441
```

Additional diagnostic plots:

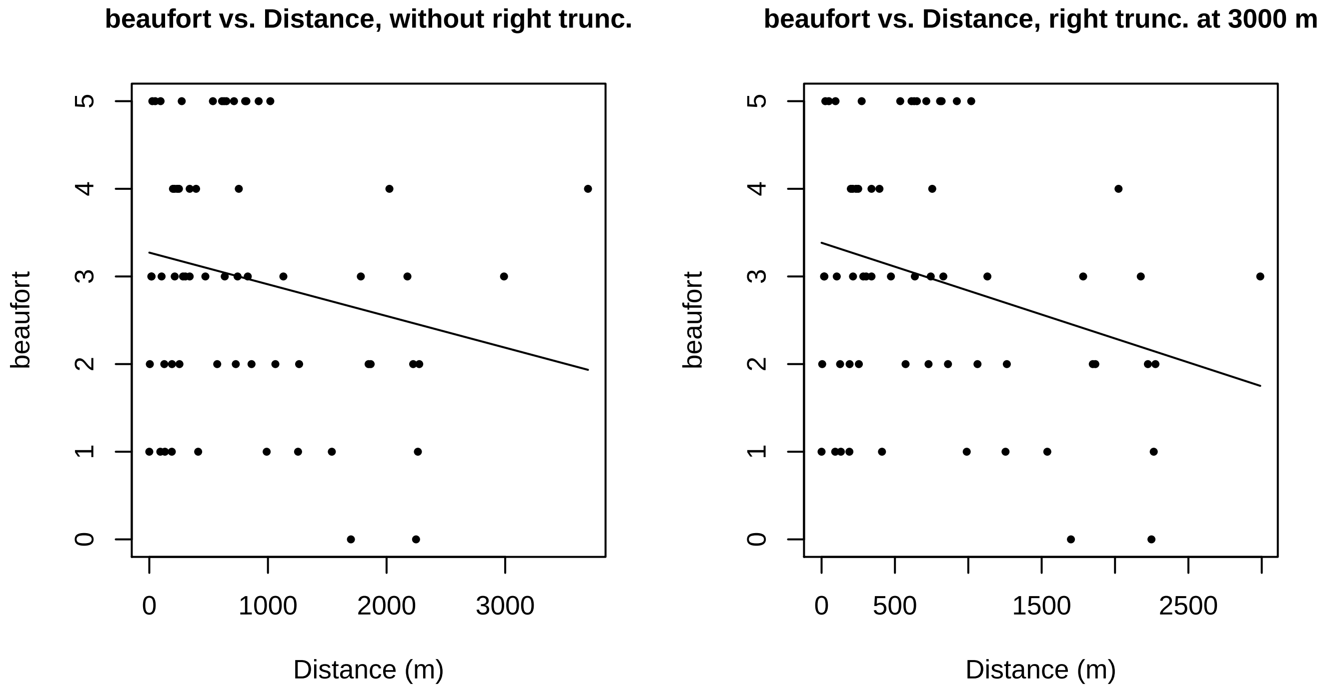

Figure 10: Scatterplots showing the relationship between Beaufort sea state and perpendicular sighting distance, for all sightings (left) and only those not right truncated (right). The line is a simple linear regression.

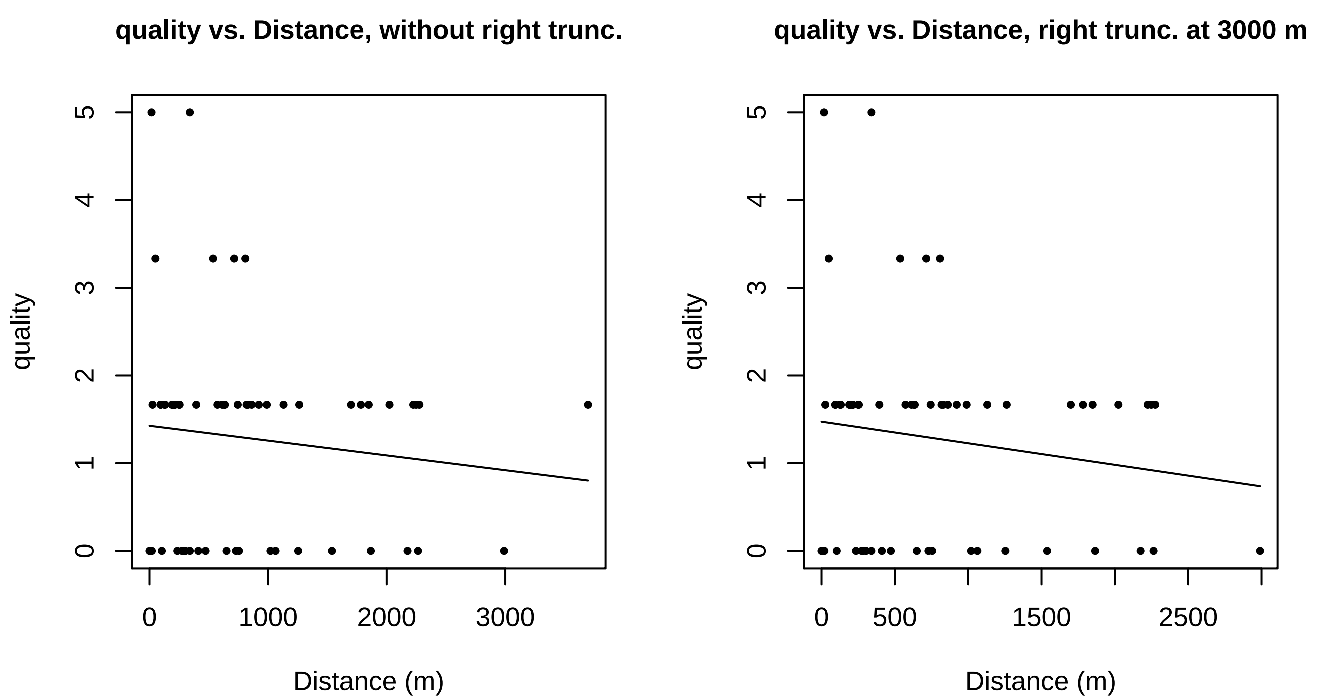

Figure 11: Scatterplots showing the relationship between the survey-specific index of the quality of observation conditions and perpendicular sighting distance, for all sightings (left) and only those not right truncated (right). Low values of the quality index correspond to better observation conditions. The line is a simple linear regression.

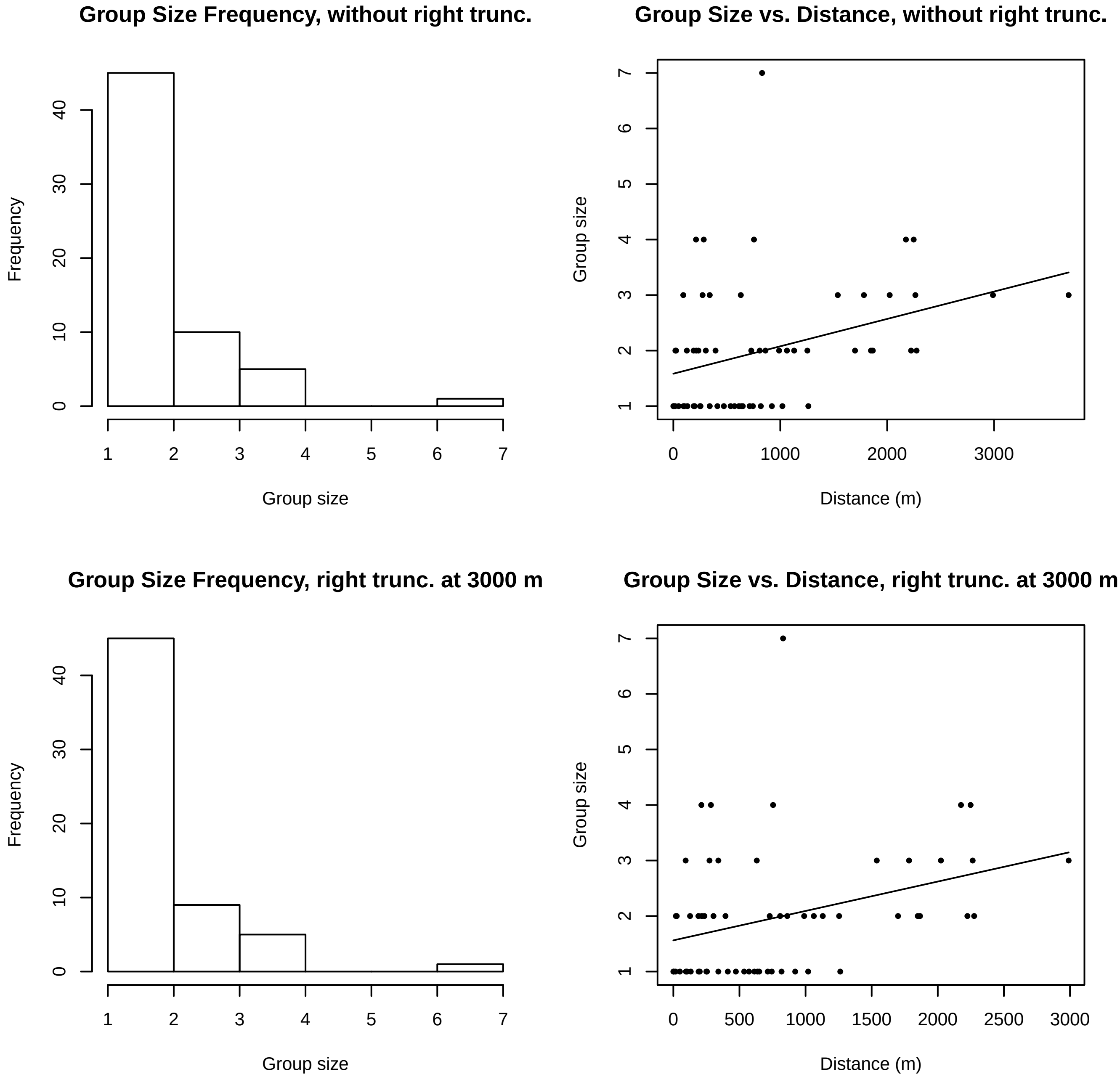

Figure 12: Histograms showing group size frequency and scatterplots showing the relationship between group size and perpendicular sighting distance, for all sightings (top row) and only those not right truncated (bottom row). In the scatterplot, the line is a simple linear regression.

SEFSC Gordon Gunter

The sightings were right truncated at 6000m.

Covariate	Description
beaufort	Beaufort sea state.
size	Estimated size (number of individuals) of the sighted group.

Table 6: Covariates tested in candidate "multi-covariate distance sampling" (MCDS) detection functions.

Key	Adjustment	Order	Covariates	Succeeded	Δ AIC	Mean ESHW (m)
hr			beaufort	Yes	0.00	2258
hr			beaufort, size	Yes	1.17	2284
hn			beaufort	Yes	1.66	2657
hr				Yes	2.76	2377
hn	cos	2		Yes	3.22	2063
hn			beaufort, size	Yes	3.45	2657
hr			size	Yes	4.10	2361
hr	poly	2		Yes	4.76	2377
hn				Yes	4.87	2512
hr	poly	4		Yes	4.90	2453
hn			size	Yes	6.25	2507
hn	herm	4		Yes	6.71	2506
hn	cos	3		Yes	6.71	2367

Table 7: Candidate detection functions for SEFSC Gordon Gunter. The first one listed was selected for the density model.

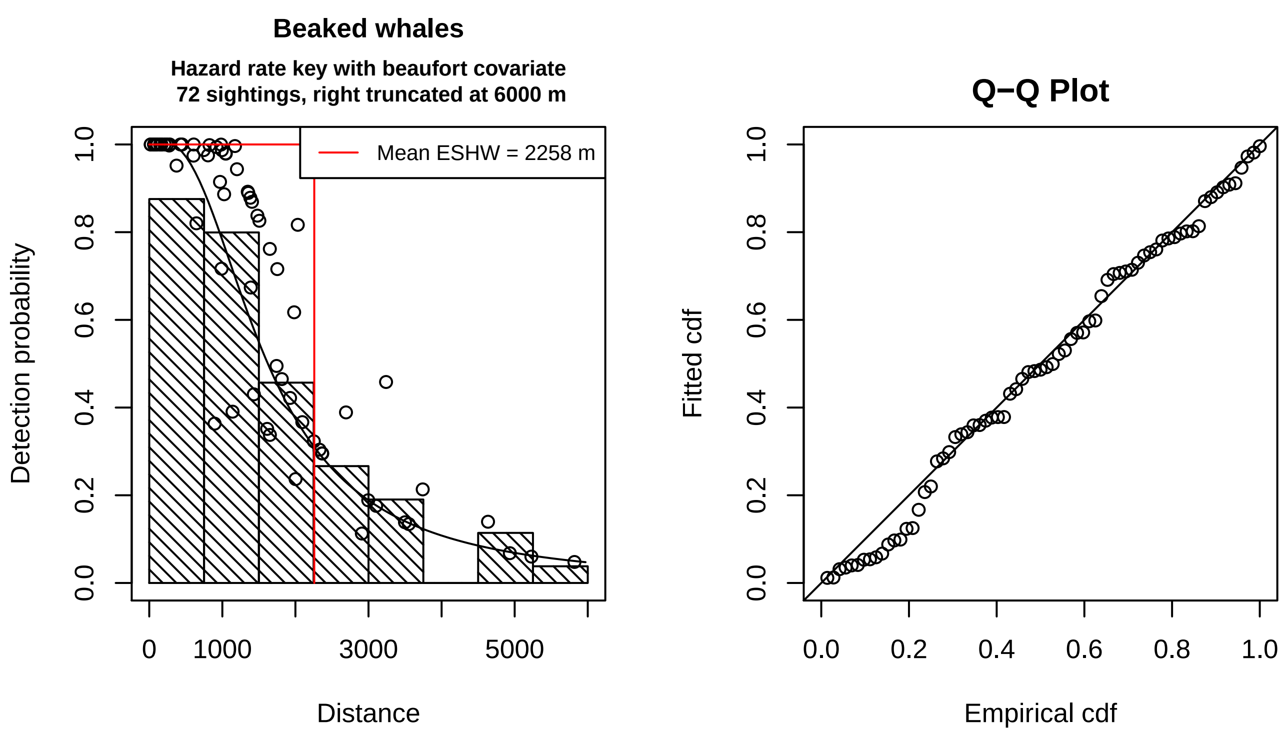

Figure 13: Detection function for SEFSC Gordon Gunter that was selected for the density model

Statistical output for this detection function:

```
Summary for ds object
```

```
Number of observations :  72
Distance range         :  0  -  6000
AIC                    :  1194.489

Detection function:
 Hazard-rate key function

Detection function parameters
Scale Coefficients:
              estimate        se
(Intercept)  7.8592898 0.3568977
beaufort    -0.2855211 0.1289825

Shape parameters:
             estimate        se
(Intercept) 0.7805475 0.2484692

                       Estimate         SE        CV
Average p             0.3425973  0.0516629 0.1507977
N in covered region 210.1592533 37.7928095 0.1798294
```

Additional diagnostic plots:

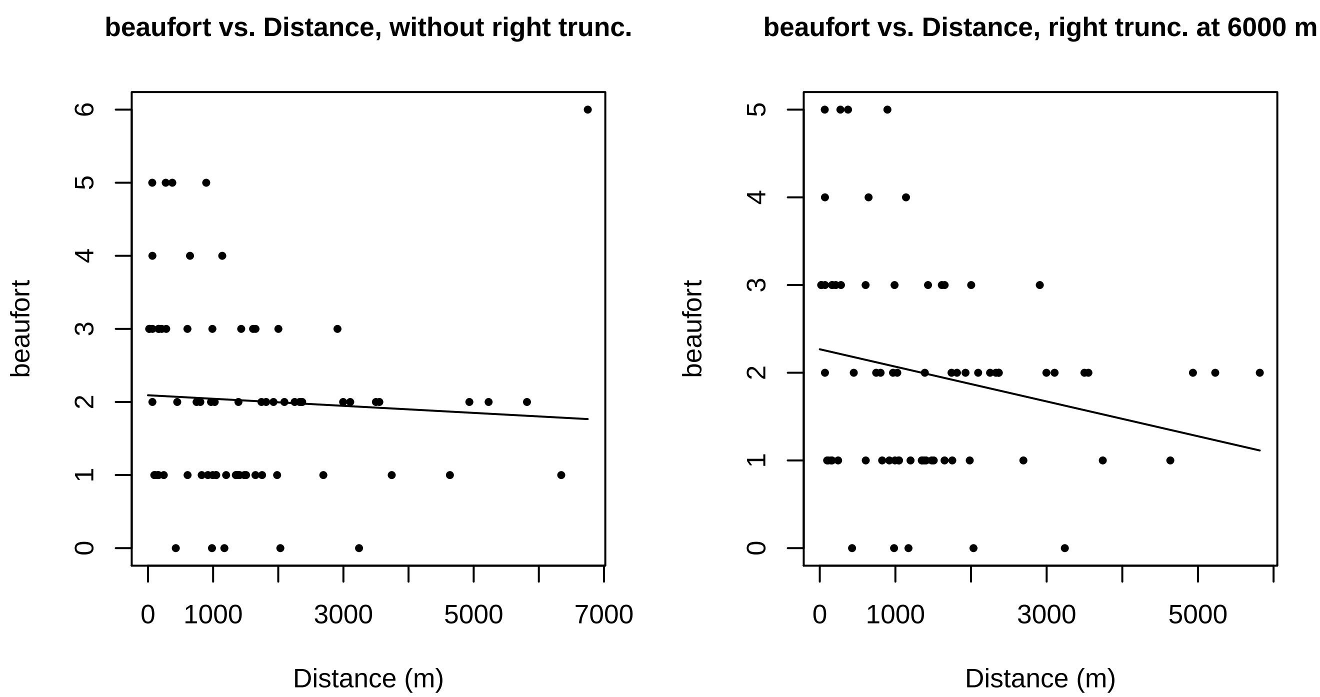

Figure 14: Scatterplots showing the relationship between Beaufort sea state and perpendicular sighting distance, for all sightings (left) and only those not right truncated (right). The line is a simple linear regression.

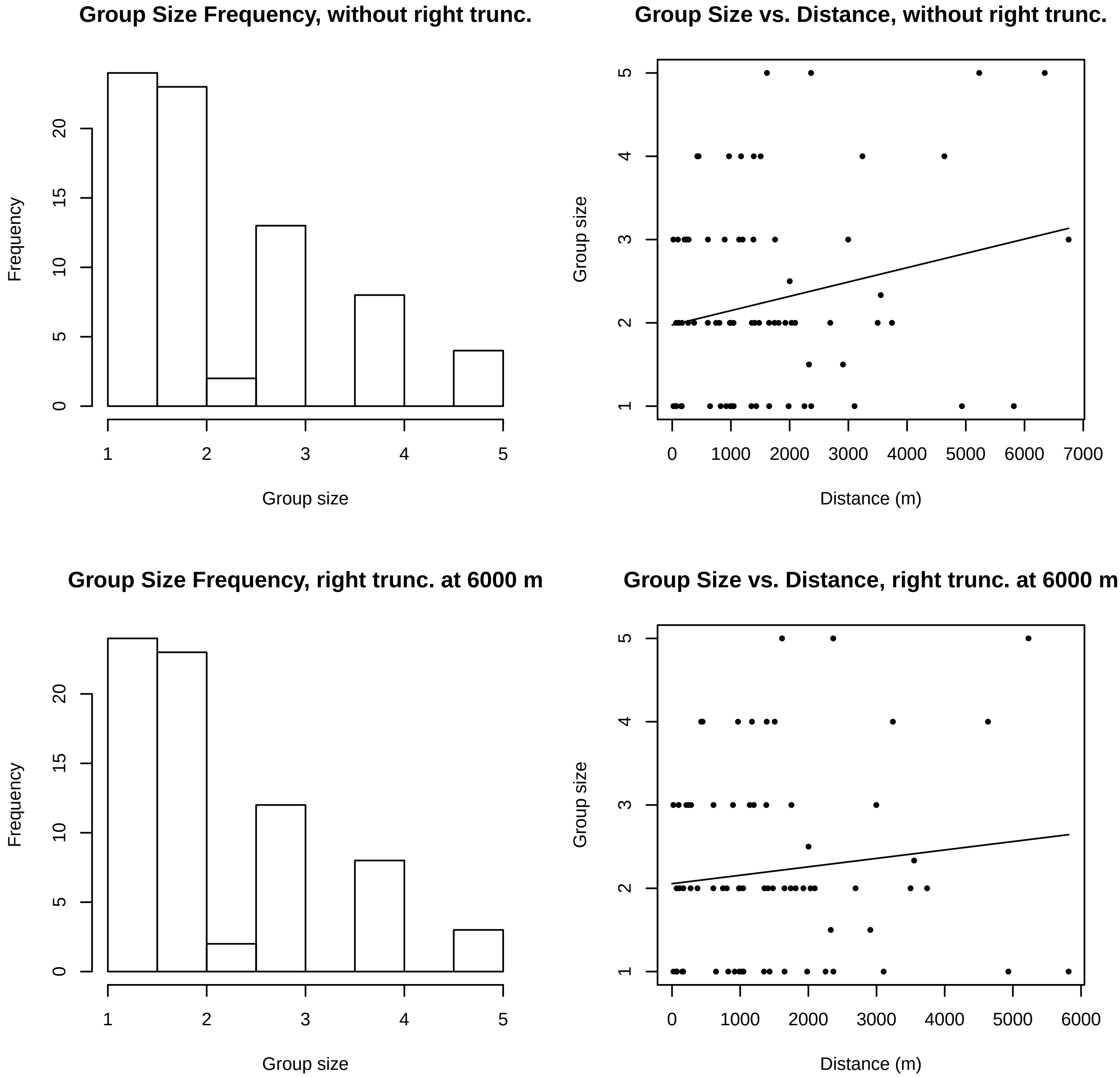

Figure 15: Histograms showing group size frequency and scatterplots showing the relationship between group size and perpendicular sighting distance, for all sightings (top row) and only those not right truncated (bottom row). In the scatterplot, the line is a simple linear regression.

Aerial Surveys

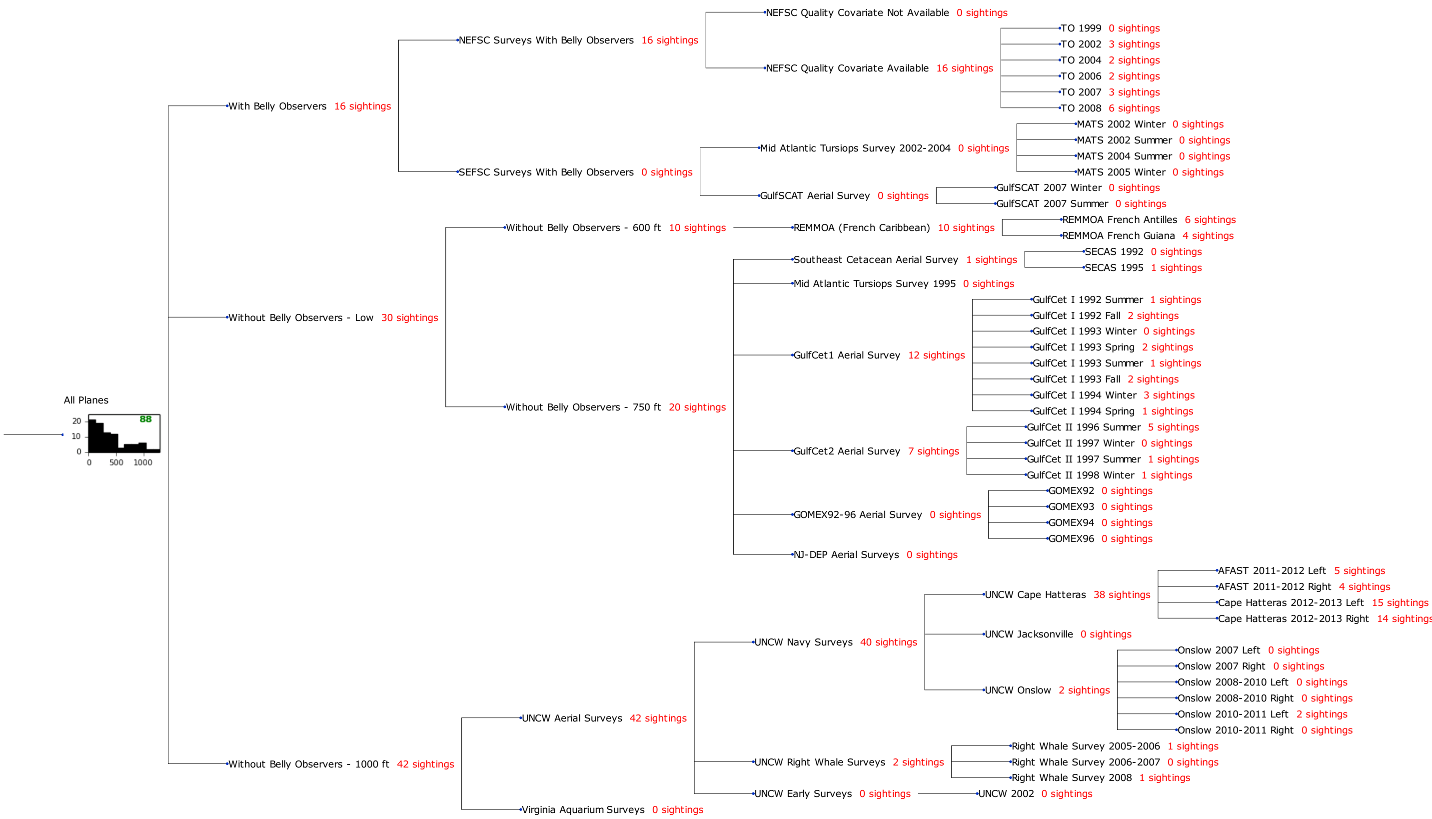

Figure 16: Detection hierarchy for aerial surveys

All Planes

The sightings were right truncated at 1500m.

Covariate	Description
beaufort	Beaufort sea state.
size	Estimated size (number of individuals) of the sighted group.

Table 8: Covariates tested in candidate "multi-covariate distance sampling" (MCDS) detection functions.

Key	Adjustment	Order	Covariates	Succeeded	Δ AIC	Mean ESHW (m)
hn	cos	3		Yes	0.00	478
hr	poly	4		Yes	2.16	479
hn	cos	2		Yes	3.05	544
hr				Yes	3.73	492
hn				Yes	4.42	647
hr			size	Yes	5.70	495
hr	poly	2		Yes	5.73	492

hn			beaufort	Yes	6.20	647
hn	herm	4		Yes	6.37	645
hr			beaufort	No		
hn			size	No		
hr			beaufort, size	No		
hn			beaufort, size	No		

Table 9: Candidate detection functions for All Planes. The first one listed was selected for the density model.

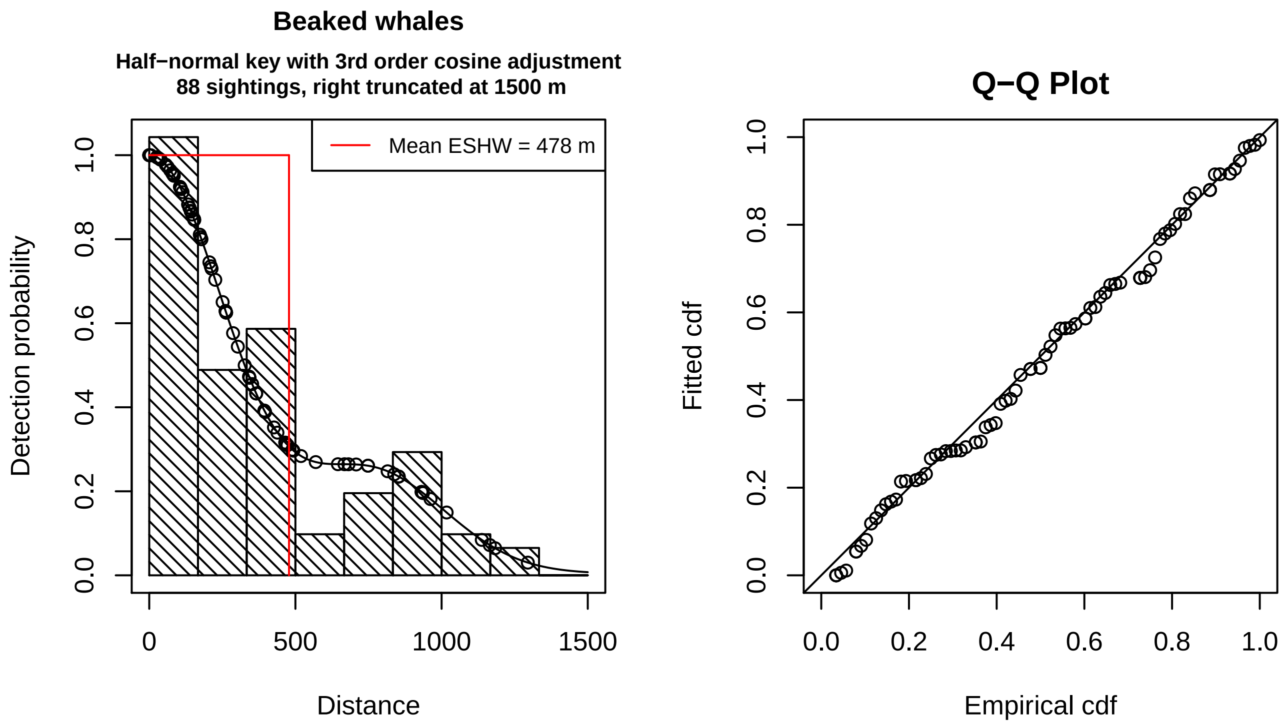

Figure 17: Detection function for All Planes that was selected for the density model

Statistical output for this detection function:

```
Summary for ds object
Number of observations :  88
Distance range         :  0  -  1500
AIC                    :  1221.593

Detection function:
 Half-normal key function with cosine adjustment term of order 3

Detection function parameters
Scale Coefficients:
            estimate         se
(Intercept) 6.257817 0.07793329

Adjustment term parameter(s):
              estimate        se
```

```
cos, order 3 0.3665265 0.1373015


Monotonicity constraints were enforced.
                      Estimate          SE        CV
Average p            0.3186994  0.03987822 0.1251280
N in covered region 276.1222435 42.23773925 0.1529675

Monotonicity constraints were enforced.
```

Additional diagnostic plots:

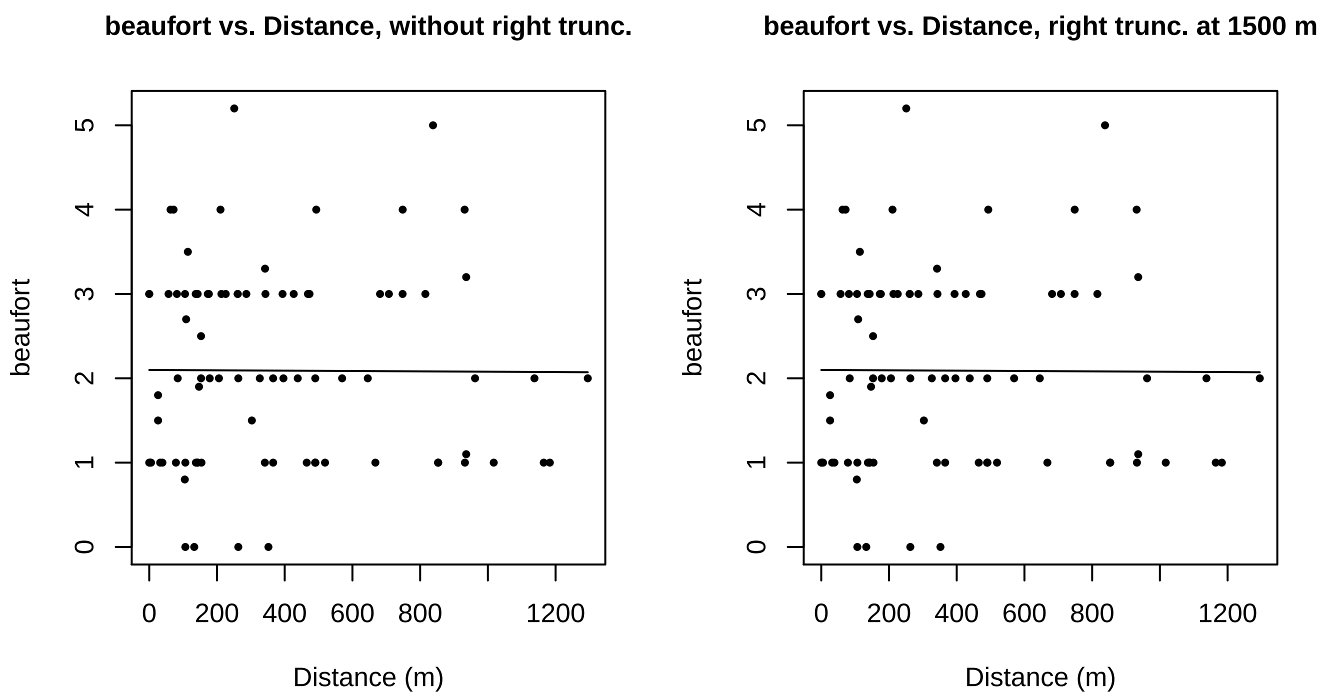

Figure 18: Scatterplots showing the relationship between Beaufort sea state and perpendicular sighting distance, for all sightings (left) and only those not right truncated (right). The line is a simple linear regression.

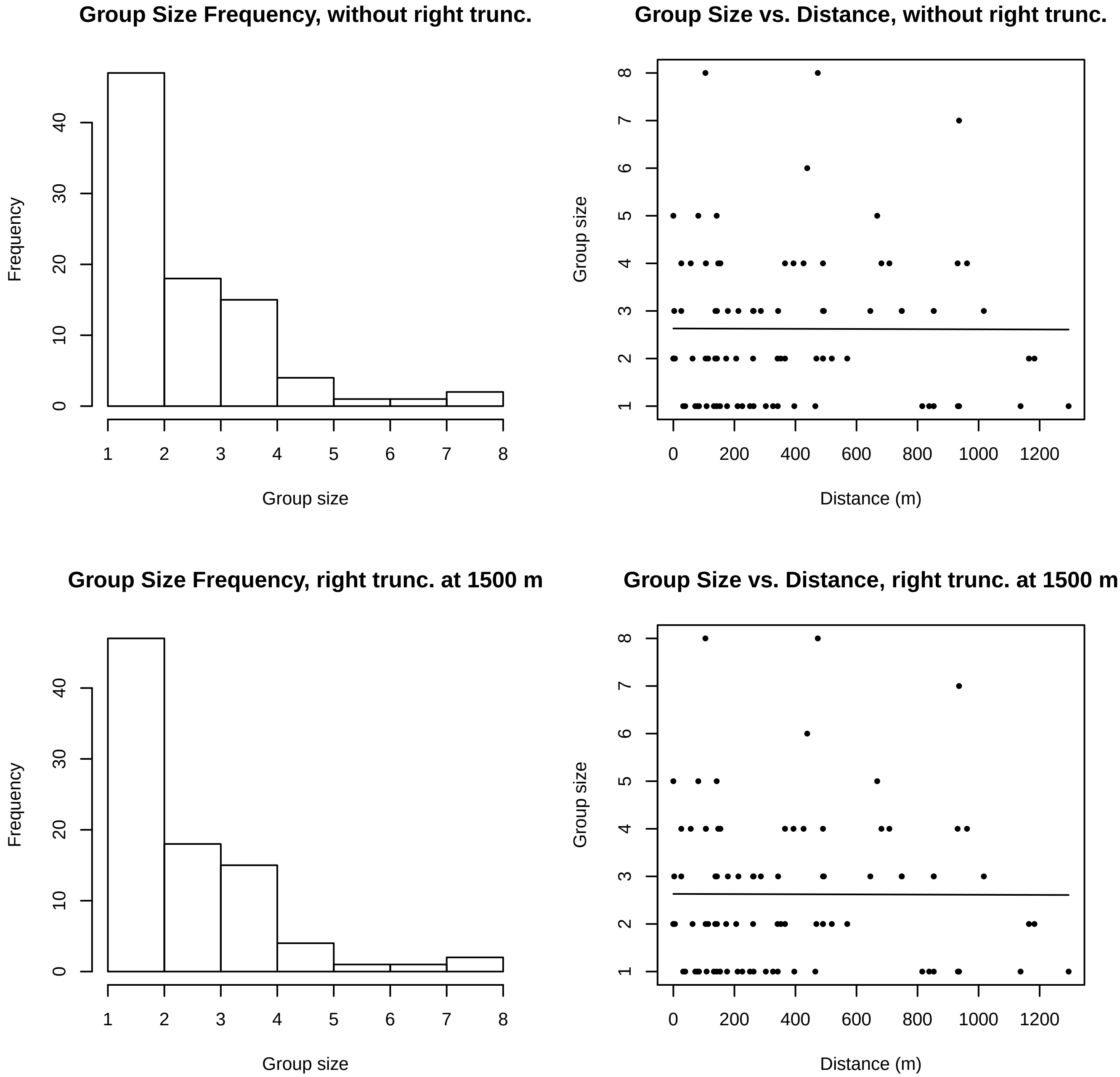

Figure 19: Histograms showing group size frequency and scatterplots showing the relationship between group size and perpendicular sighting distance, for all sightings (top row) and only those not right truncated (bottom row). In the scatterplot, the line is a simple linear regression.

g(0) Estimates

Platform	Surveys	Group Size	*g(0)*	Biases Addressed	Source
Shipboard	All	Any	0.23	Both	Barlow (1999)
Aerial	All	Any	0.074	Availability	Barlow (1999)

Table 10: Estimates of *g(0)* used in this density model.

No survey-specific g(0) estimates were available for our shipboard surveys. Instead, we relied on results from Barlow's (1999) simulation model, who modeled g(0) for Ziphius cavirostris (Cuvier's beaked whale) and the Mesoplodon genus (several species) from shipboard surveys that utilized 25x binoculars, reporting g(0) estimates of 0.23 and 0.45, respectively, accounting for both availability and perception bias. But because roughly 75% of our beaked whale sightings had ambiguous species identifications, we were unable to build species-specific models, making the use of Barlow's estimates problematic: which should we use? We selected the Ziphius cavirostris estimate, the lower of the two, as 88% of our definitive beaked whale sightings were for Ziphius cavirostris. Also, Barlow's simulation assumed a dive model in which the mean dive duration of Mesoplodon spp. was 20.4 min and Ziphius cavirostris was 28.6 min. These durations were based on shipboard observations of 27 and 43 dive cycles, respectively. Research since that time has shown that foraging beaked whales exhibit a complex dive pattern in which a deep dive of 45-60 min to followed by several shallower dives of roughly 20 min (Baird et al. 2006, Tyack et al. 2006, Schorr et al. 2014). If this pattern were accounted for in Barlow's simulation, the g(0) estimates would decrease; our choice of the lower g(0) value was precautionary against that eventuality.

No estimate of g(0) was available in the literature for beaked whales sighted on aerial surveys. Beaked whales are long-diving animals (Barlow 1999), thus availability bias is likely to be substantial. Utilizing equation (3) of Carretta et al. (2000) (which follows Barlow et al. 1988), we computed the availability bias component of g(0) from the mean surface and dive intervals (126 s and 28.6 min) for Ziphius cavirostris reported by Barlow (1999). (Our choice of Ziphius cavirostris was consistent with the shipboard g(0) we used). Our estimate (g(0)=0.074) is similar to the mean daytime % time in surface bouts (7.0%) reported by Schorr et al. (2014) for 3732 hr of dive data collected from 8 Ziphius cavirostris, the largest database of beaked whale dive records yet published. We did not incorporate an estimate of perception bias or account for the periodic deep dives that last 45-60 min, thus our g(0) estimate is likely to be biased high.

Density Models

Beaked whales are difficult for observers to identify at sea (Waring et al. 2014). Although some of the more recent surveys in our database provided full species identifications for some sightings, or at least determined the identification to the genus level, the large majority of sightings available over the study period reported "unidentified beaked whale" as the taxonomic identification. At a review meeting, NOAA coauthors confirmed that these sightings corresponded to beaked whales of either the Mesoplodon or Ziphius genera. This model, therefore, is of the guild comprising the two Mesoplodon species and the one Ziphius species that inhabit the Gulf of Mexico: Blainville's beaked whale (M. densirostris), Gervais' beaked whale (M. europaeus), and Cuvier's beaked whale (Z. cavirostris).

Beaked whales are generally believed to occupy similar foraging niches, undertaking long, deep dives to hunt for mesopelagic squid and fish (Madsen et al. 2014). Beaked whales are often found in deep water near high-relief bathymetric features, such as slopes, canyons, and escarpments (MacLeod and D'Amico 2006), where preferred prey are believed to aggregate (Moors-Murphy 2014). All of the sightings reported by our surveys occurred over the continental slope or the abyss; none were reported over the continental shelf. Compared to other cetacean species, little is known about beaked whales and our literature review did not yield any descriptions of seasonal movements for these species. Given this off-shelf distribution with no knowledge of seasonal patterns, we fitted a year-round model to off-shelf waters, defined here as those deeper than the 100m isobath.

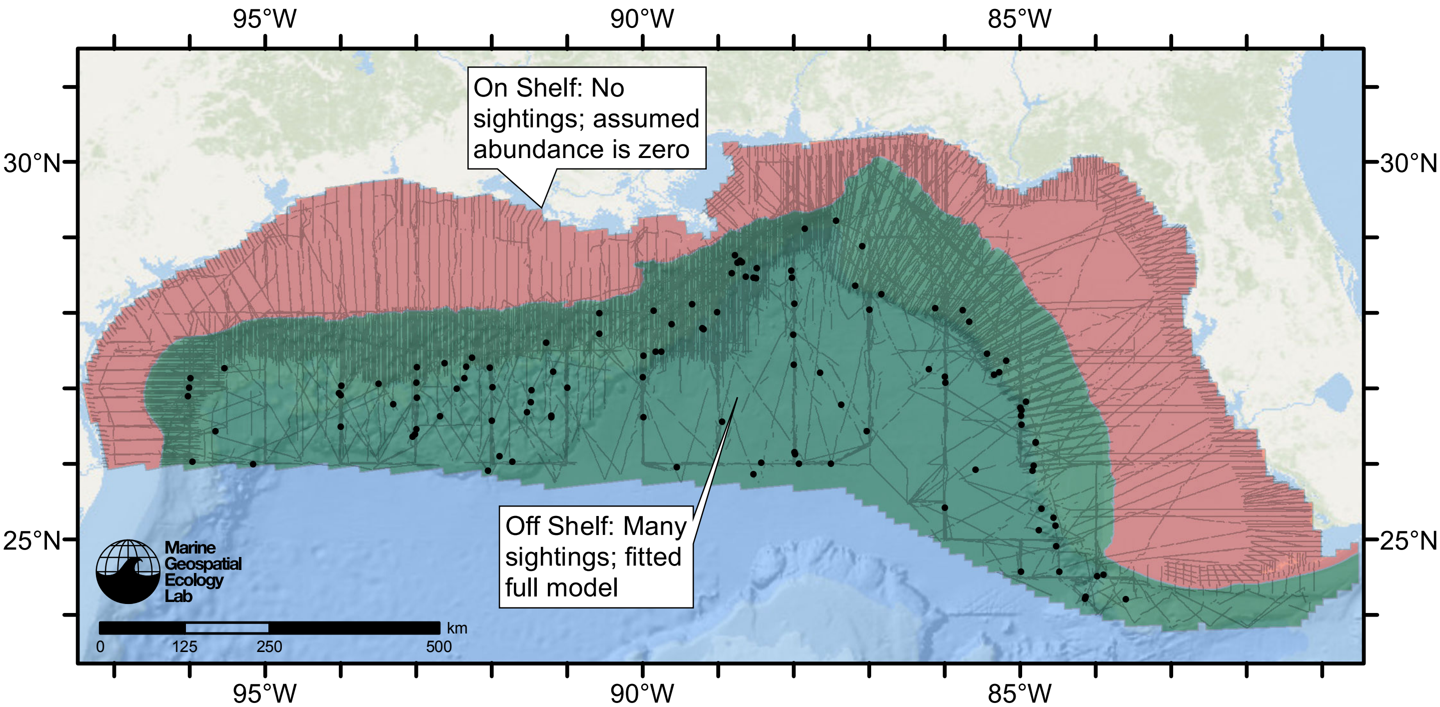

Figure 20: Beaked whales density model schematic. All on-effort sightings are shown, including those that were truncated when detection functions were fitted.

Climatological Model

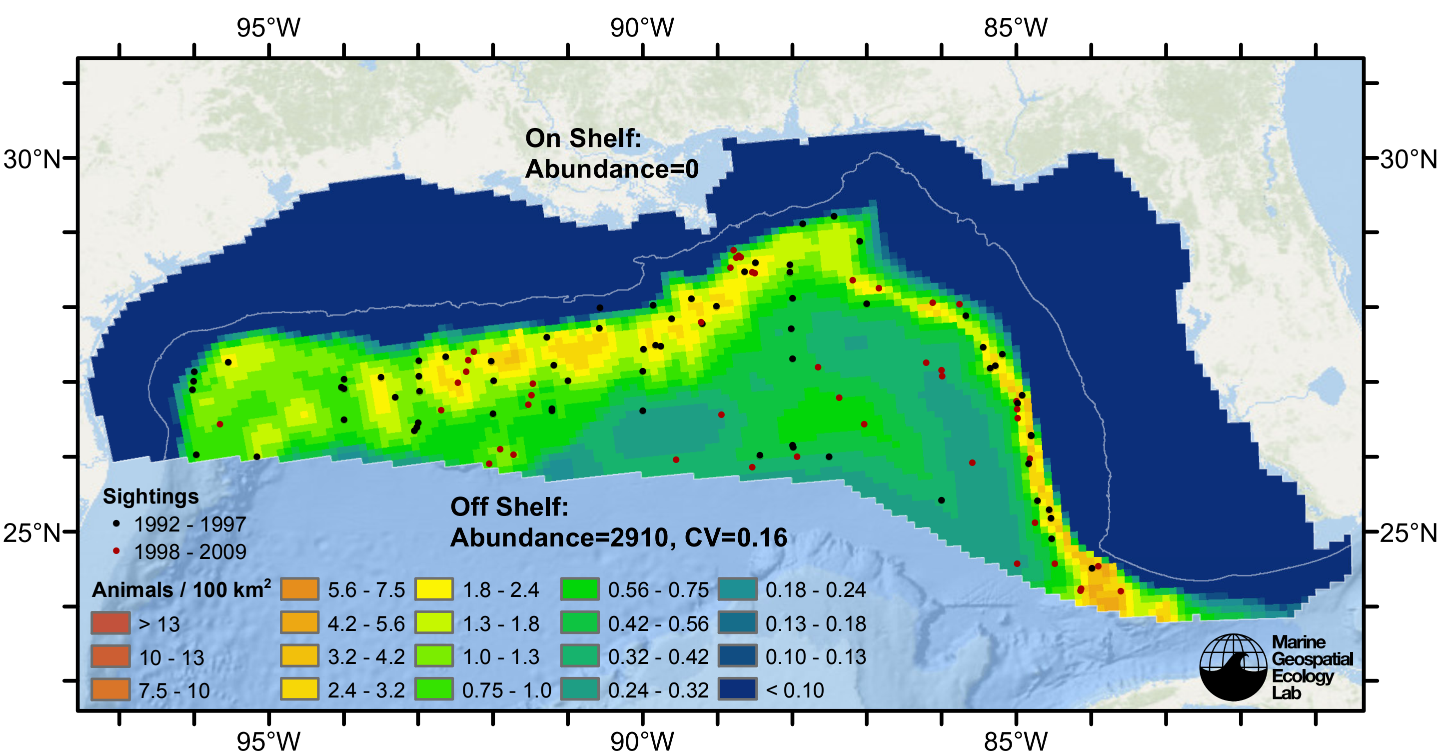

Figure 21: Beaked whales density predicted by the climatological model that explained the most deviance. Pixels are 10x10 km. The legend gives the estimated individuals per pixel; breaks are logarithmic. Abundance for each region was computed by summing the density cells occuring in that region.

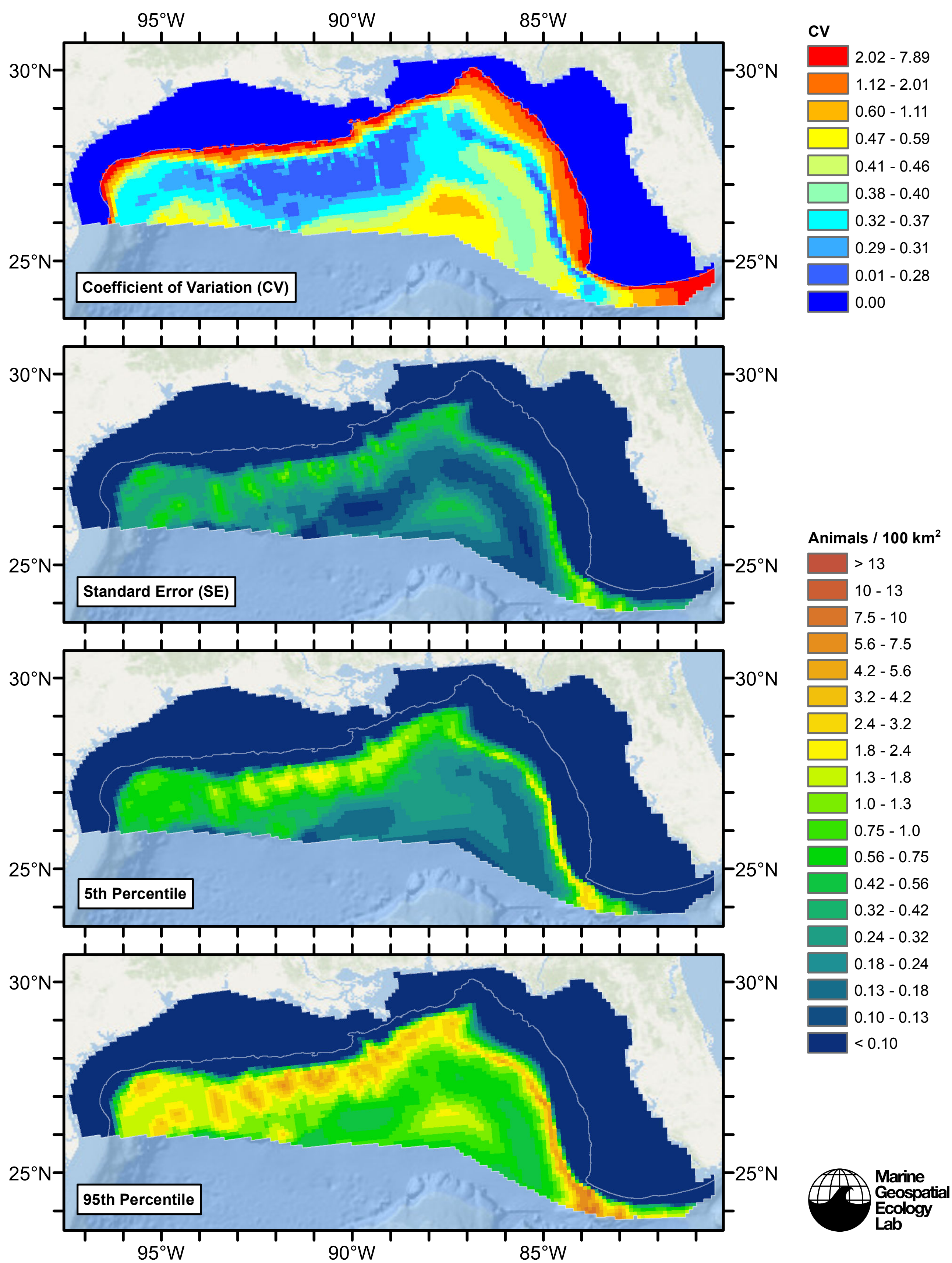

Figure 22: Estimated uncertainty for the climatological model that explained the most deviance. These estimates only incorporate the statistical uncertainty estimated for the spatial model (by the R mgcv package). They do not incorporate uncertainty in the detection functions, g(0) estimates, predictor variables, and so on.

Off Shelf

Statistical output

```
Rscript.exe: This is mgcv 1.8-3. For overview type 'help("mgcv-package")'.


Family: Tweedie(p=1.385)
Link function: log

Formula:
abundance ~ offset(log(area_km2)) + s(log10(Depth), bs = "ts",
    k = 5) + s(sqrt(DistToCanyon), bs = "ts", k = 5) + s(I(ClimDistToAEddy4/1000),
    bs = "ts", k = 5) + s(I(ClimDistToCEddy4/1000), bs = "ts",
    k = 5) + s(log10(ClimCumVGPM90), bs = "ts", k = 5)

Parametric coefficients:
            Estimate Std. Error t value Pr(>|t|)
(Intercept)  -7.0296     0.4209   -16.7   <2e-16 ***
---
Signif. codes:  0 '***' 0.001 '**' 0.01 '*' 0.05 '.' 0.1 ' ' 1

Approximate significance of smooth terms:
                             edf Ref.df     F  p-value
s(log10(Depth))            2.8451      4 9.485 2.88e-09 ***
s(sqrt(DistToCanyon))      2.0545      4 1.844  0.01689 *
s(I(ClimDistToAEddy4/1000)) 0.9562      4 2.162  0.00197 **
s(I(ClimDistToCEddy4/1000)) 2.5858      4 2.125  0.01733 *
s(log10(ClimCumVGPM90))     0.9208      4 2.195  0.00168 **
---
Signif. codes:  0 '***' 0.001 '**' 0.01 '*' 0.05 '.' 0.1 ' ' 1

R-sq.(adj) =  -0.00445   Deviance explained = 16.2%
-REML = 1125.8  Scale est. = 89.335    n = 14455

All predictors were significant. This is the final model.
Creating term plots.
Diagnostic output from gam.check():

Method: REML   Optimizer: outer newton
full convergence after 11 iterations.
Gradient range [-0.0001947868,0.0001469301]
(score 1125.794 & scale 89.33465).
Hessian positive definite, eigenvalue range [0.1797679,390.0099].
Model rank =  21 / 21

Basis dimension (k) checking results. Low p-value (k-index<1) may
indicate that k is too low, especially if edf is close to k'.

                              k'   edf k-index p-value
s(log10(Depth))            4.000 2.845   0.521    0.00
s(sqrt(DistToCanyon))      4.000 2.055   0.613    0.04
s(I(ClimDistToAEddy4/1000)) 4.000 0.956   0.608    0.01
s(I(ClimDistToCEddy4/1000)) 4.000 2.586   0.595    0.00
s(log10(ClimCumVGPM90))     4.000 0.921   0.612    0.02

Predictors retained during the model selection procedure: Depth, DistToCanyon, ClimDistToAEddy4,
ClimDistToCEddy4, ClimCumVGPM90
```

Predictors dropped during the model selection procedure: Slope, ClimSST, ClimDistToFront2, ClimTKE

Model term plots

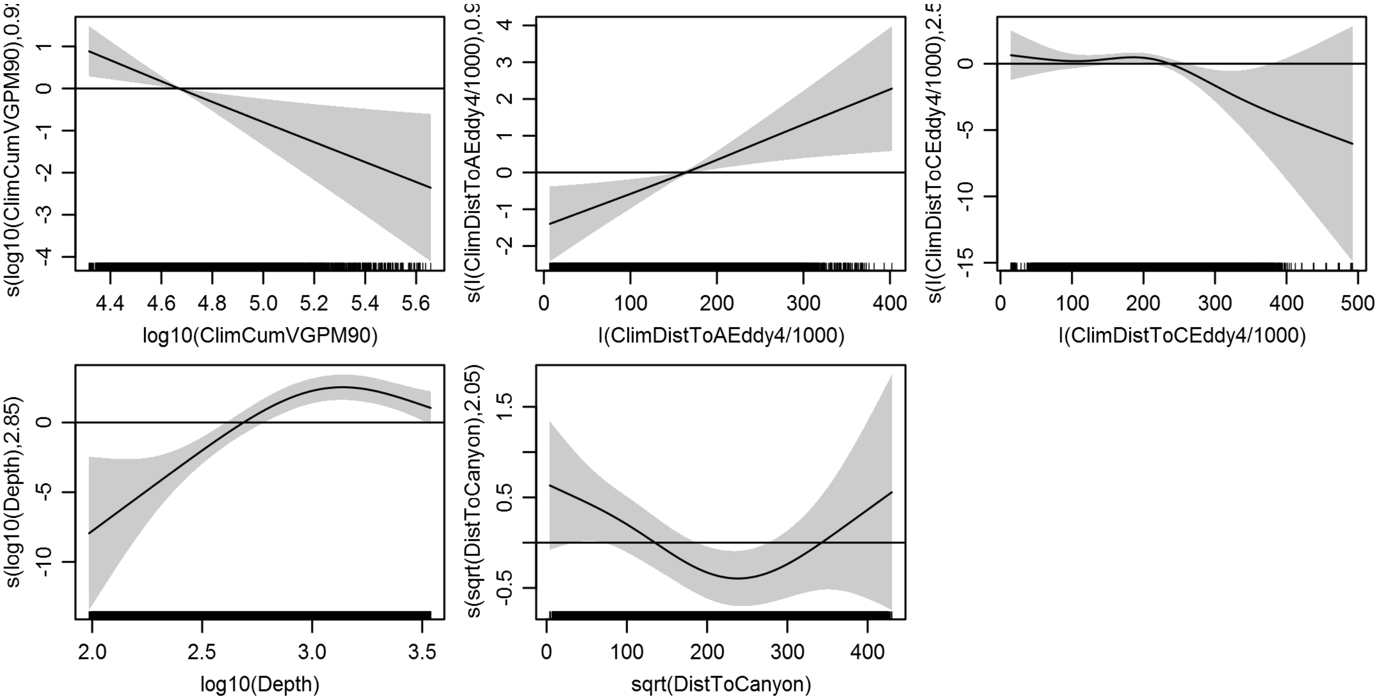

Diagnostic plots

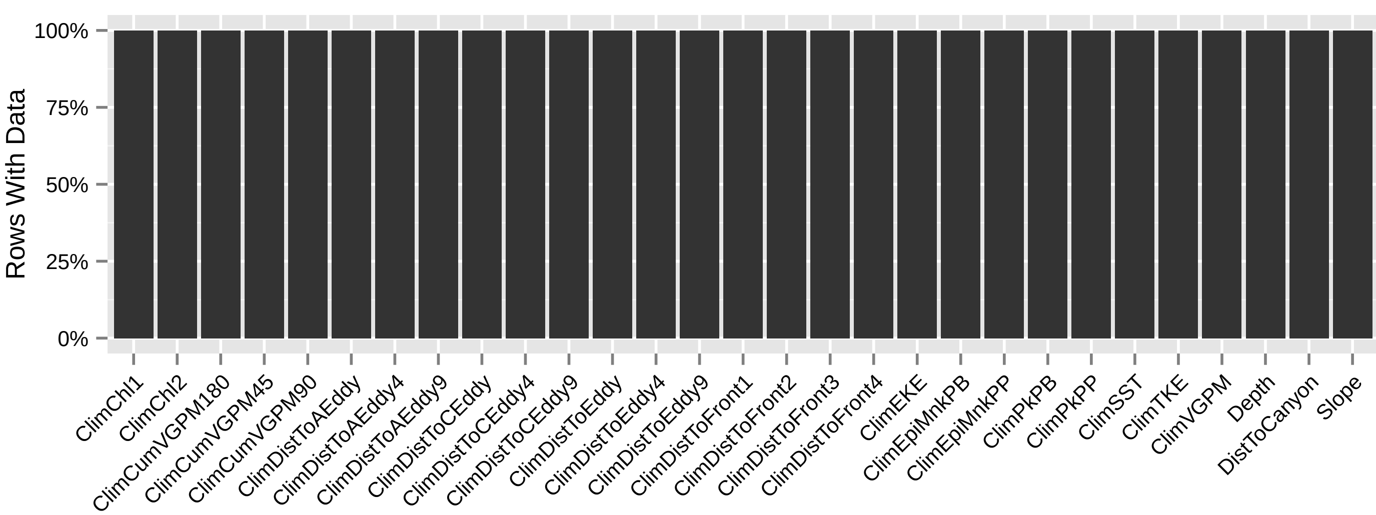

Figure 23: Segments with predictor values for the Beaked whales Climatological model, Off Shelf. This plot is used to assess how many segments would be lost by including a given predictor in a model.

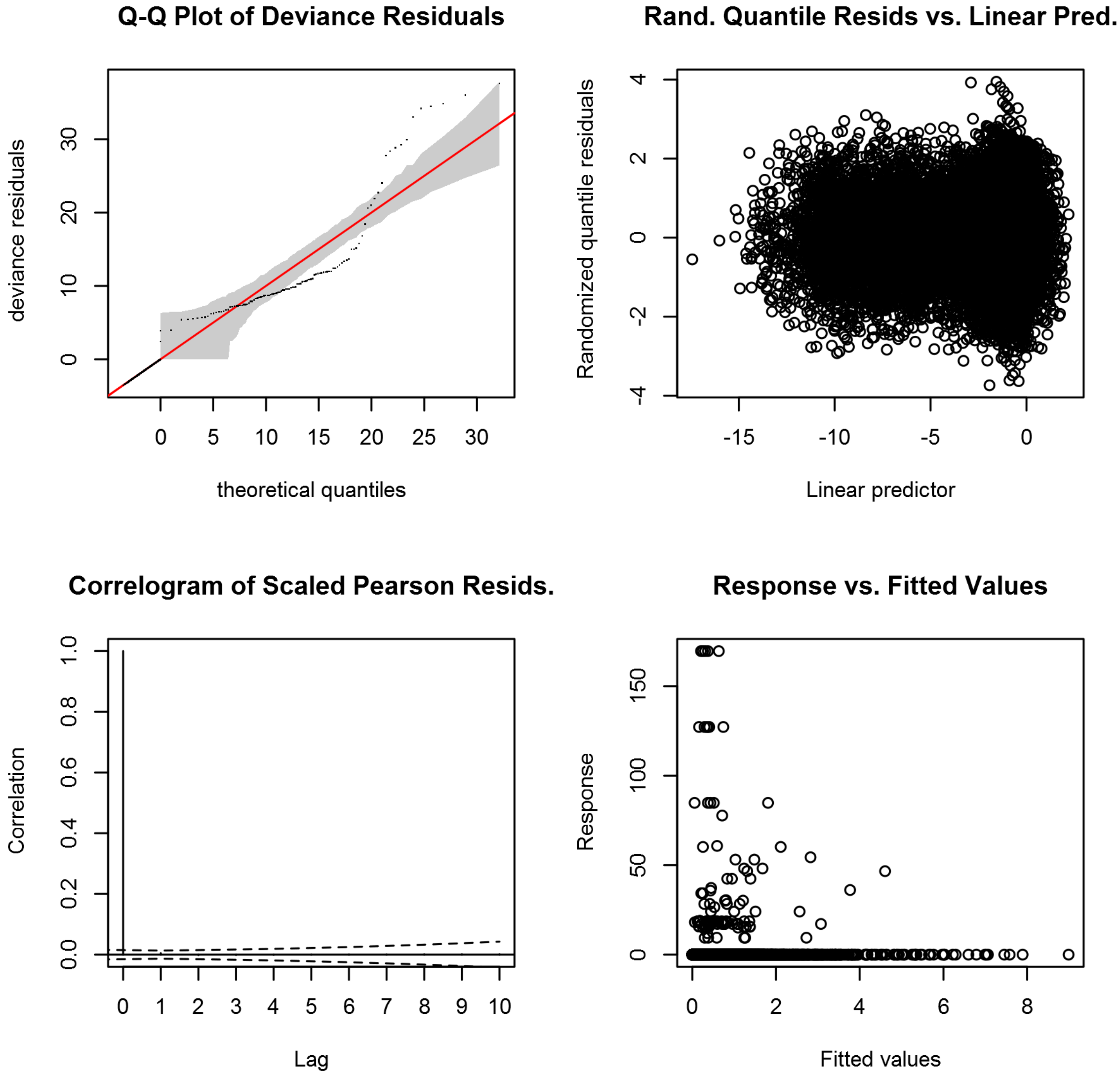

Figure 24: Statistical diagnostic plots for the Beaked whales Climatological model, Off Shelf.

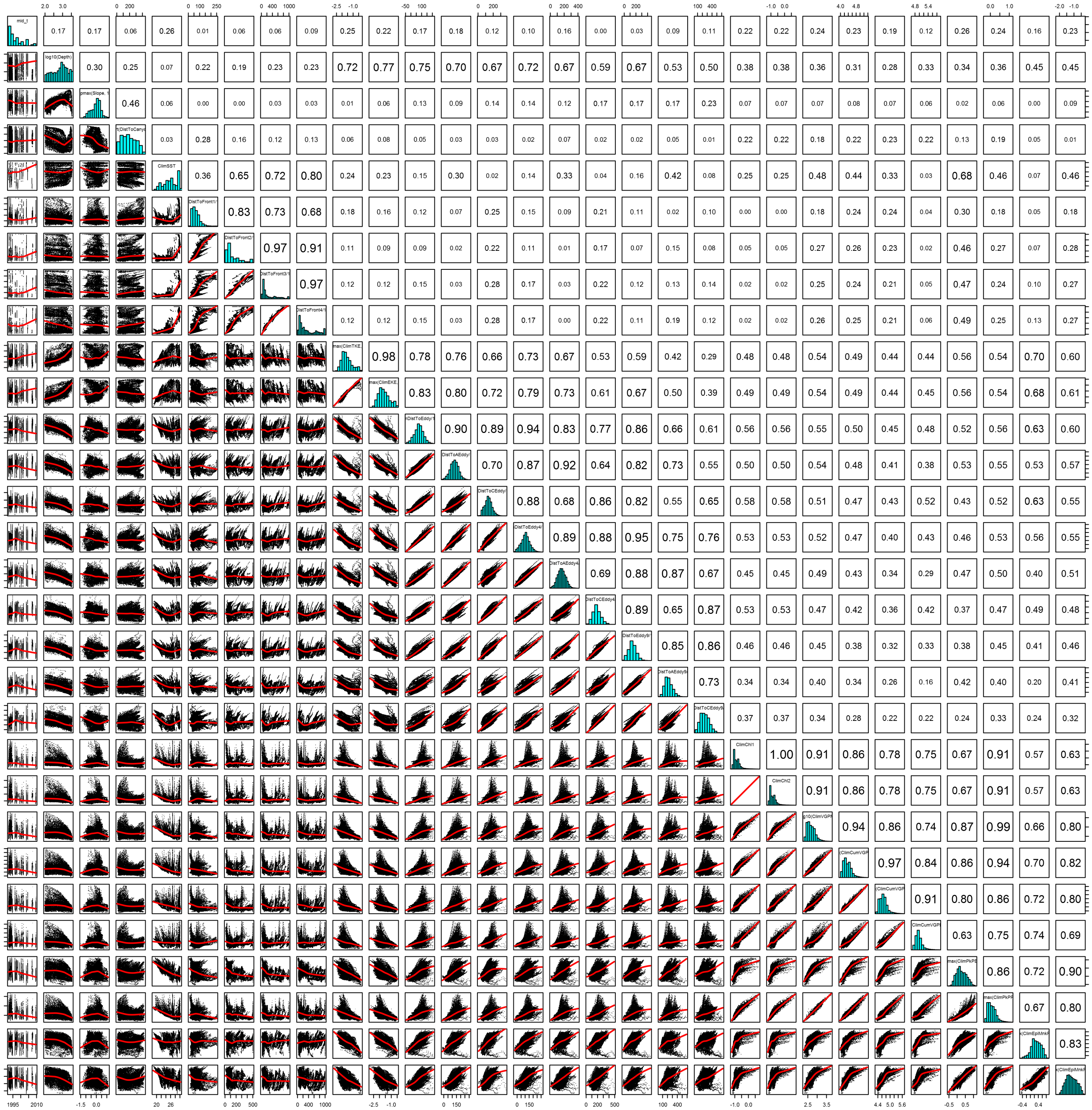

Figure 25: Scatterplot matrix for the Beaked whales Climatological model, Off Shelf. This plot is used to inspect the distribution of predictors (via histograms along the diagonal), simple correlation between predictors (via pairwise Pearson coefficients above the diagonal), and linearity of predictor correlations (via scatterplots below the diagonal). This plot is best viewed at high magnification.

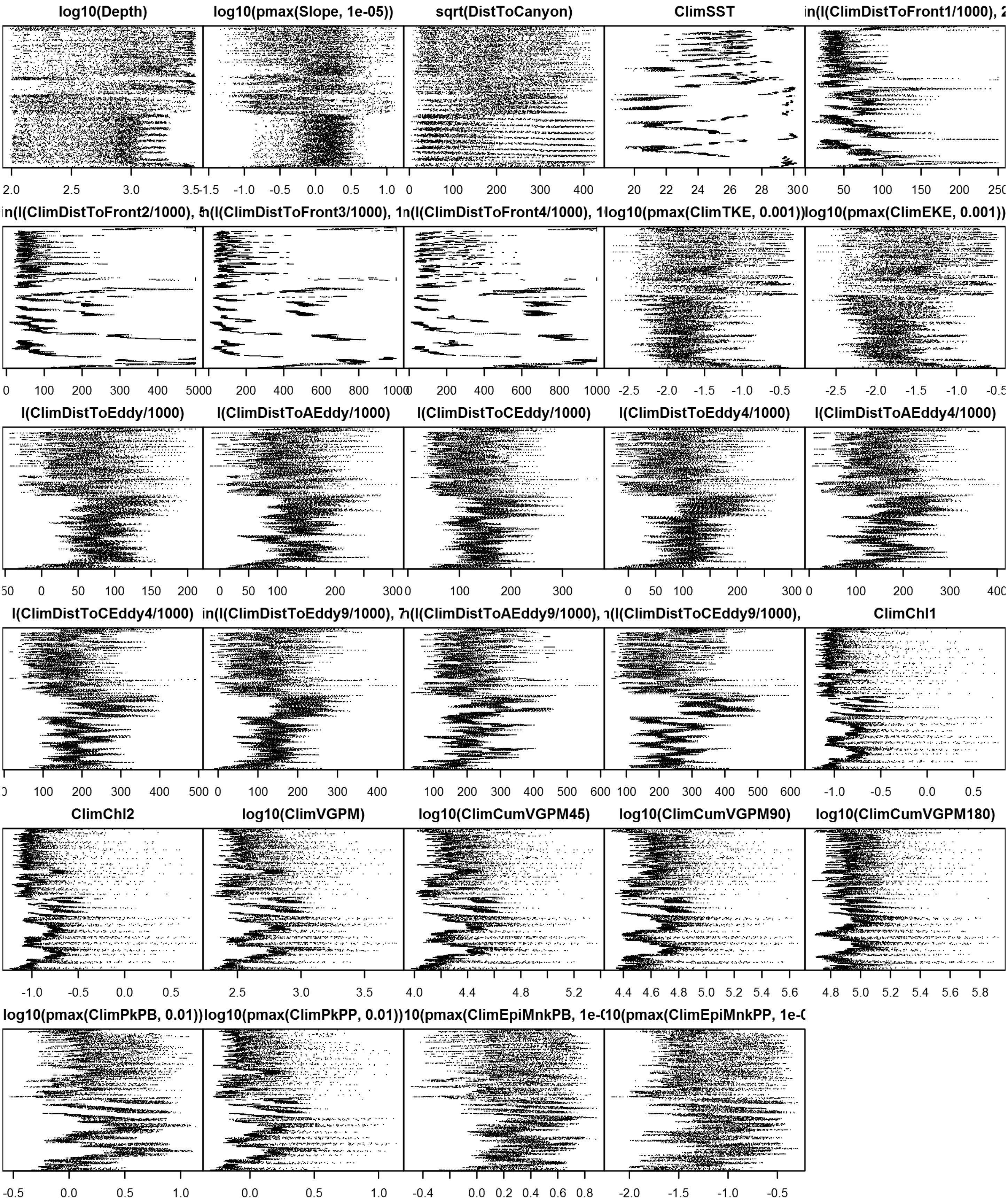

Figure 26: Dotplot for the Beaked whales Climatological model, Off Shelf. This plot is used to check for suspicious patterns and outliers in the data. Points are ordered vertically by transect ID, sequentially in time.

On Shelf

Density assumed to be 0 in this region.

Contemporaneous Model

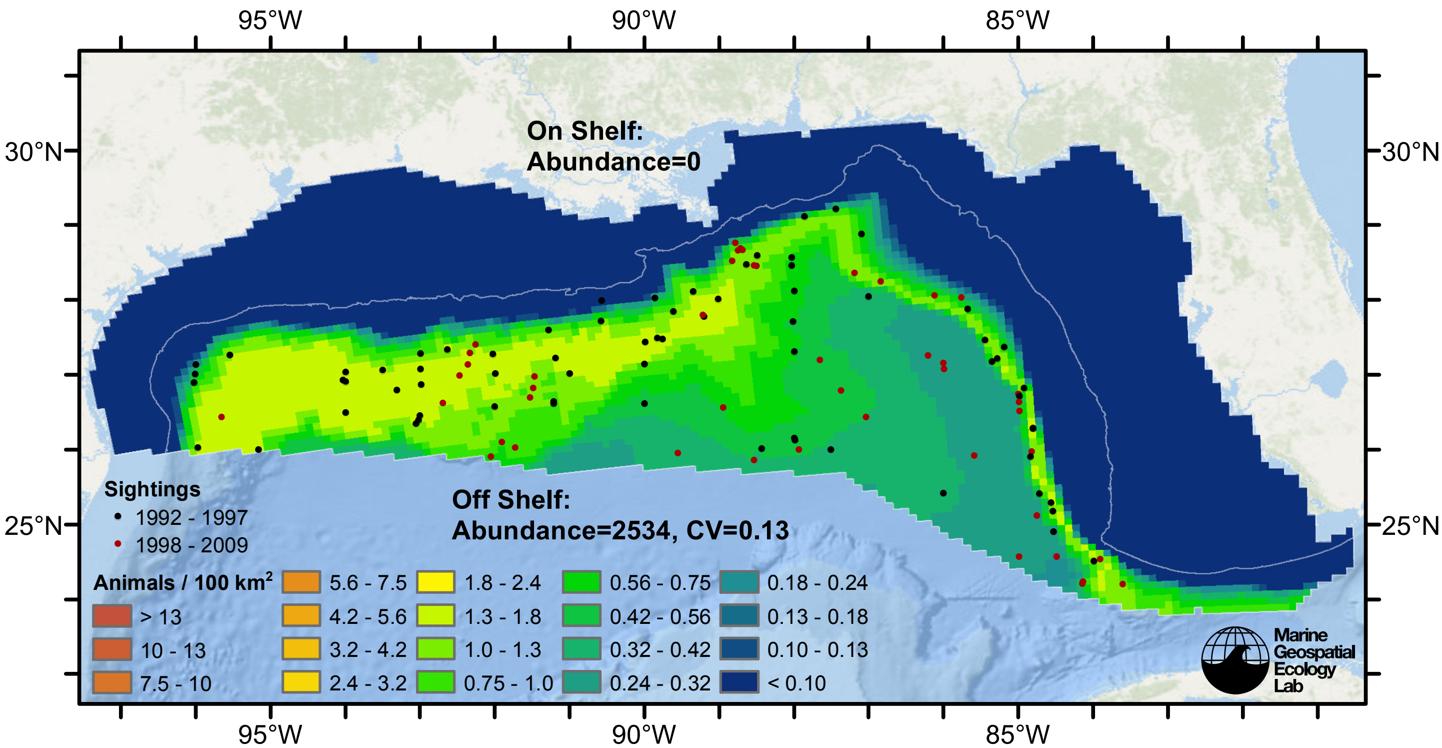

Figure 27: Beaked whales density predicted by the contemporaneous model that explained the most deviance. Pixels are 10x10 km. The legend gives the estimated individuals per pixel; breaks are logarithmic. Abundance for each region was computed by summing the density cells occuring in that region.

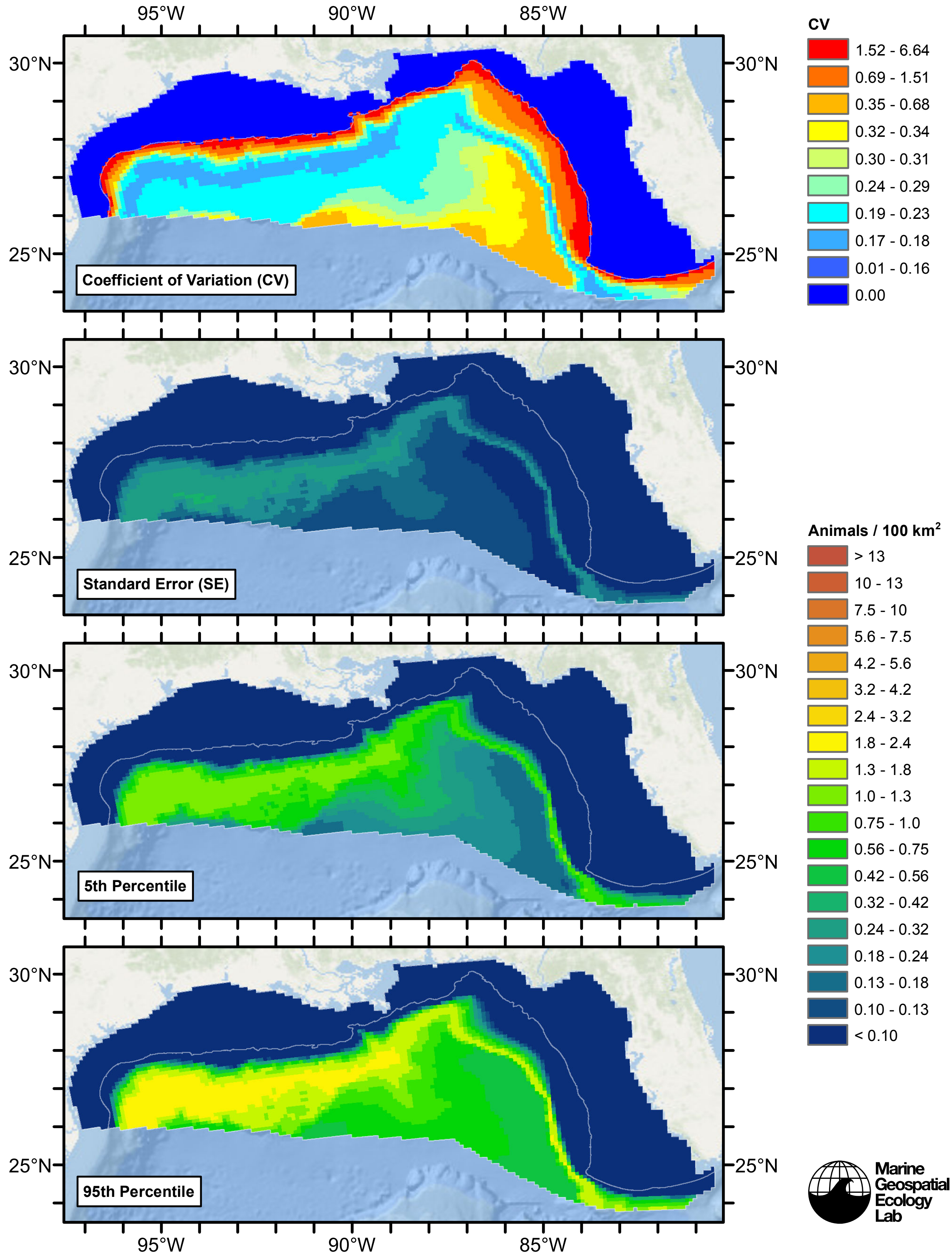

Figure 28: Estimated uncertainty for the contemporaneous model that explained the most deviance. These estimates only incorporate the statistical uncertainty estimated for the spatial model (by the R mgcv package). They do not incorporate uncertainty in the detection functions, g(0) estimates, predictor variables, and so on.

Off Shelf

Statistical output

```
Rscript.exe: This is mgcv 1.8-3. For overview type 'help("mgcv-package")'.


Family: Tweedie(p=1.364)
Link function: log

Formula:
abundance ~ offset(log(area_km2)) + s(log10(Depth), bs = "ts",
    k = 5) + s(I(DistToCEddy4/1000), bs = "ts", k = 5)

Parametric coefficients:
            Estimate Std. Error t value Pr(>|t|)
(Intercept)  -6.6084     0.3753  -17.61   <2e-16 ***
---
Signif. codes:  0 '***' 0.001 '**' 0.01 '*' 0.05 '.' 0.1 ' ' 1

Approximate significance of smooth terms:
                           edf Ref.df      F  p-value
s(log10(Depth))         2.8859      4 10.904 1.81e-10 ***
s(I(DistToCEddy4/1000)) 0.8501      4  1.222   0.0155 *
---
Signif. codes:  0 '***' 0.001 '**' 0.01 '*' 0.05 '.' 0.1 ' ' 1

R-sq.(adj) =  -0.00141   Deviance explained = 10.3%
-REML = 1020.3  Scale est. = 83.22     n = 12354

All predictors were significant. This is the final model.
Creating term plots.
Diagnostic output from gam.check():

Method: REML   Optimizer: outer newton
full convergence after 11 iterations.
Gradient range [-4.367778e-05,3.550607e-05]
(score 1020.28 & scale 83.2198).
Hessian positive definite, eigenvalue range [0.3473984,376.5385].
Model rank =  9 / 9

Basis dimension (k) checking results. Low p-value (k-index<1) may
indicate that k is too low, especially if edf is close to k'.

                           k'   edf k-index p-value
s(log10(Depth))         4.000 2.886   0.595    0.00
s(I(DistToCEddy4/1000)) 4.000 0.850   0.664    0.04

Predictors retained during the model selection procedure: Depth, DistToCEddy4

Predictors dropped during the model selection procedure: Slope, DistToCanyon, SST, DistToFront4,
TKE, DistToAEddy4
```

Model term plots

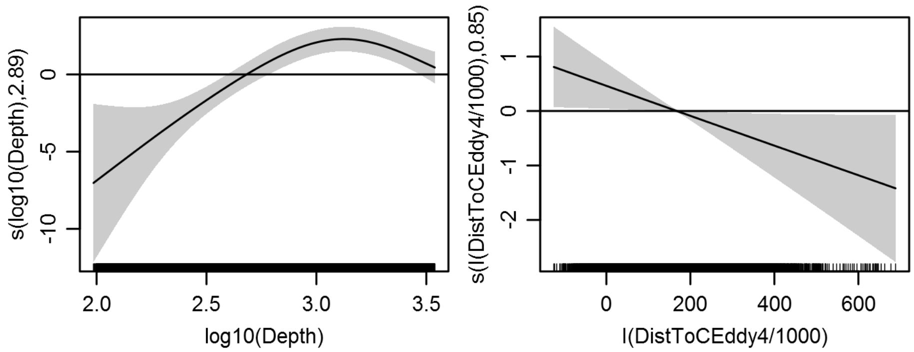

Diagnostic plots

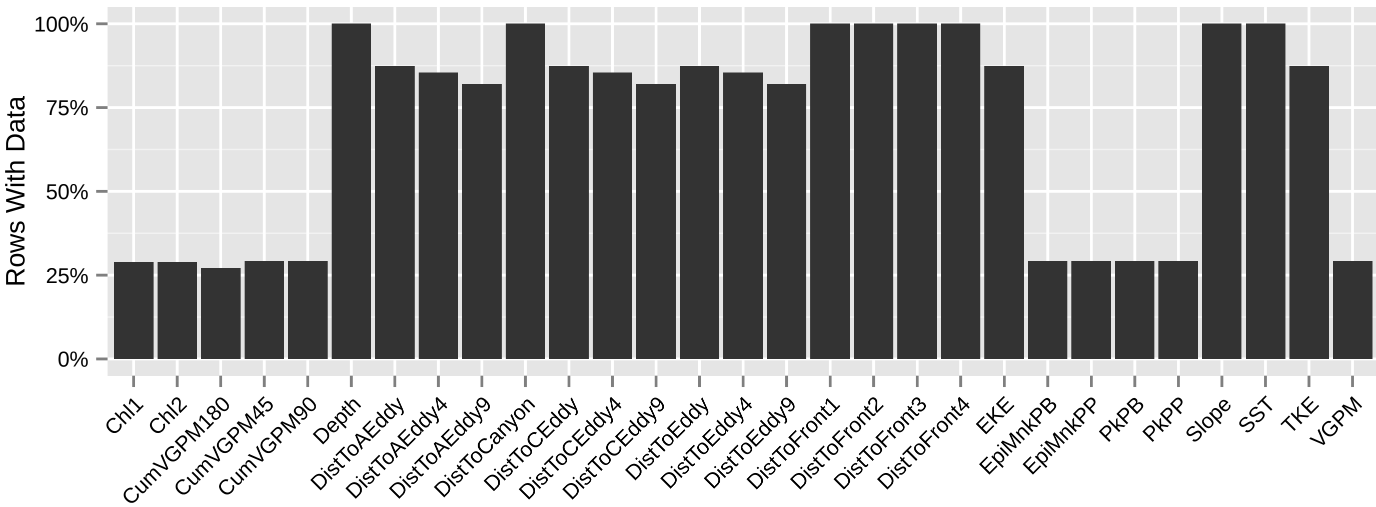

Figure 29: Segments with predictor values for the Beaked whales Contemporaneous model, Off Shelf. This plot is used to assess how many segments would be lost by including a given predictor in a model.

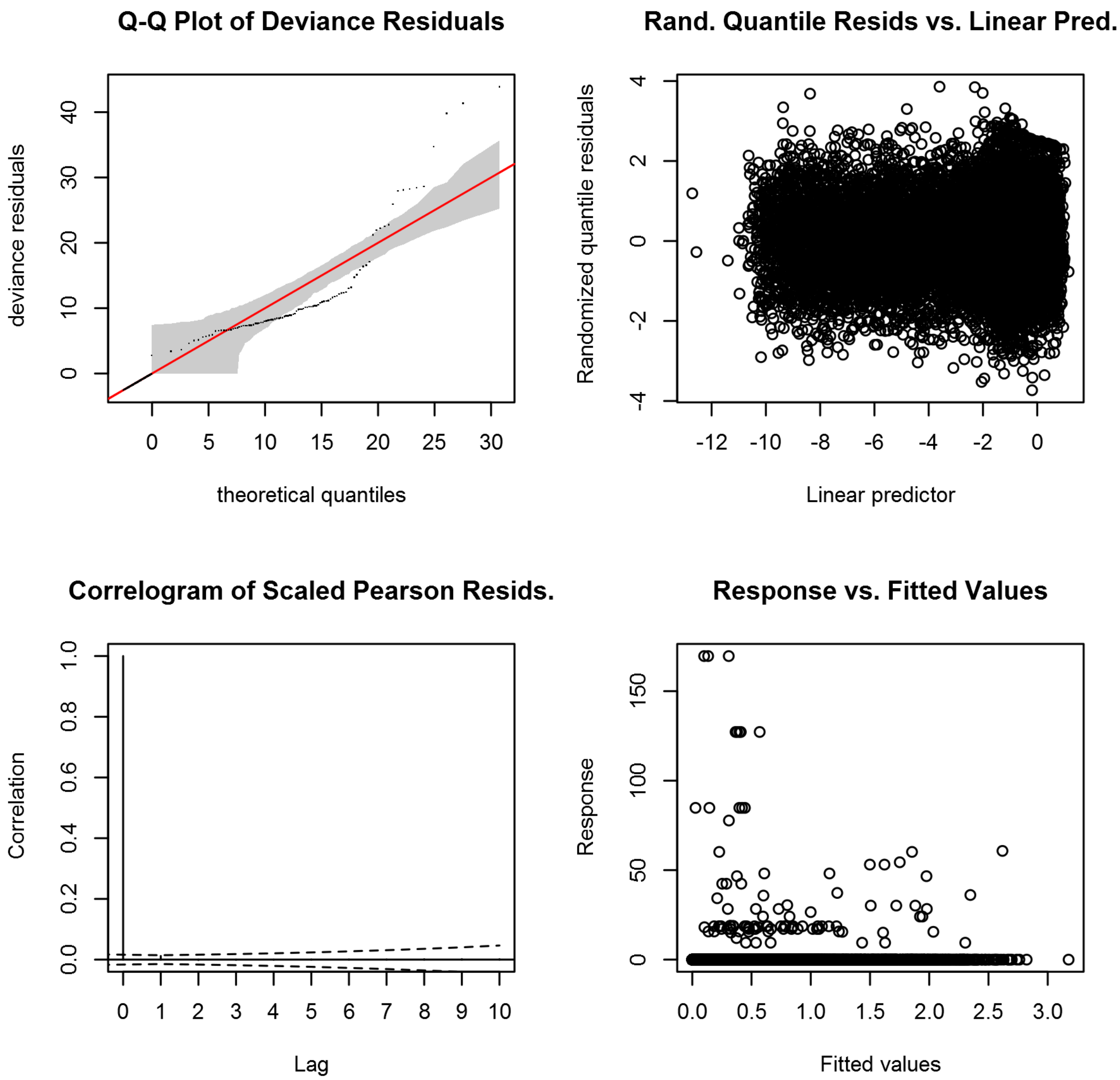

Figure 30: Statistical diagnostic plots for the Beaked whales Contemporaneous model, Off Shelf.

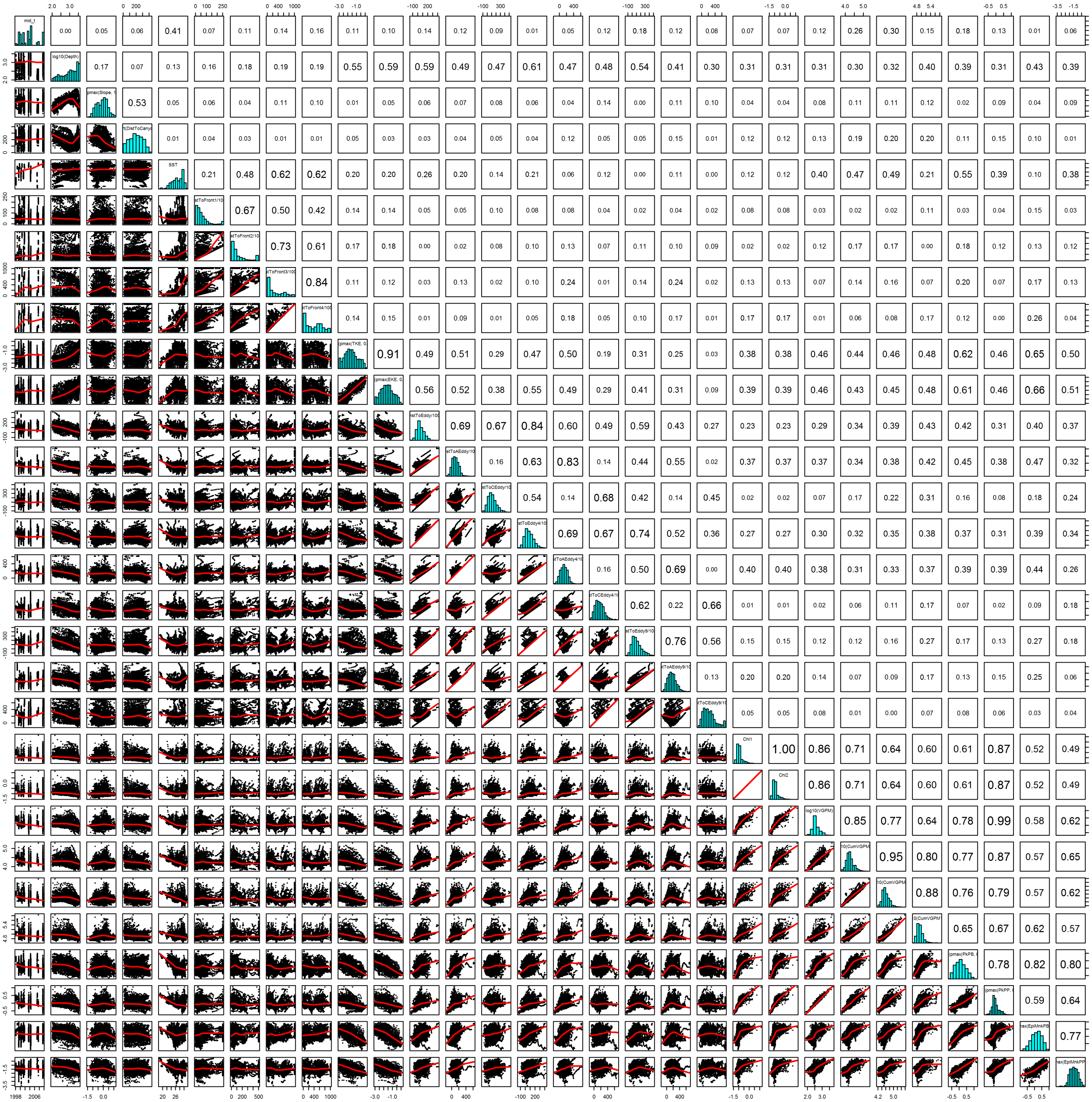

Figure 31: Scatterplot matrix for the Beaked whales Contemporaneous model, Off Shelf. This plot is used to inspect the distribution of predictors (via histograms along the diagonal), simple correlation between predictors (via pairwise Pearson coefficients above the diagonal), and linearity of predictor correlations (via scatterplots below the diagonal). This plot is best viewed at high magnification.

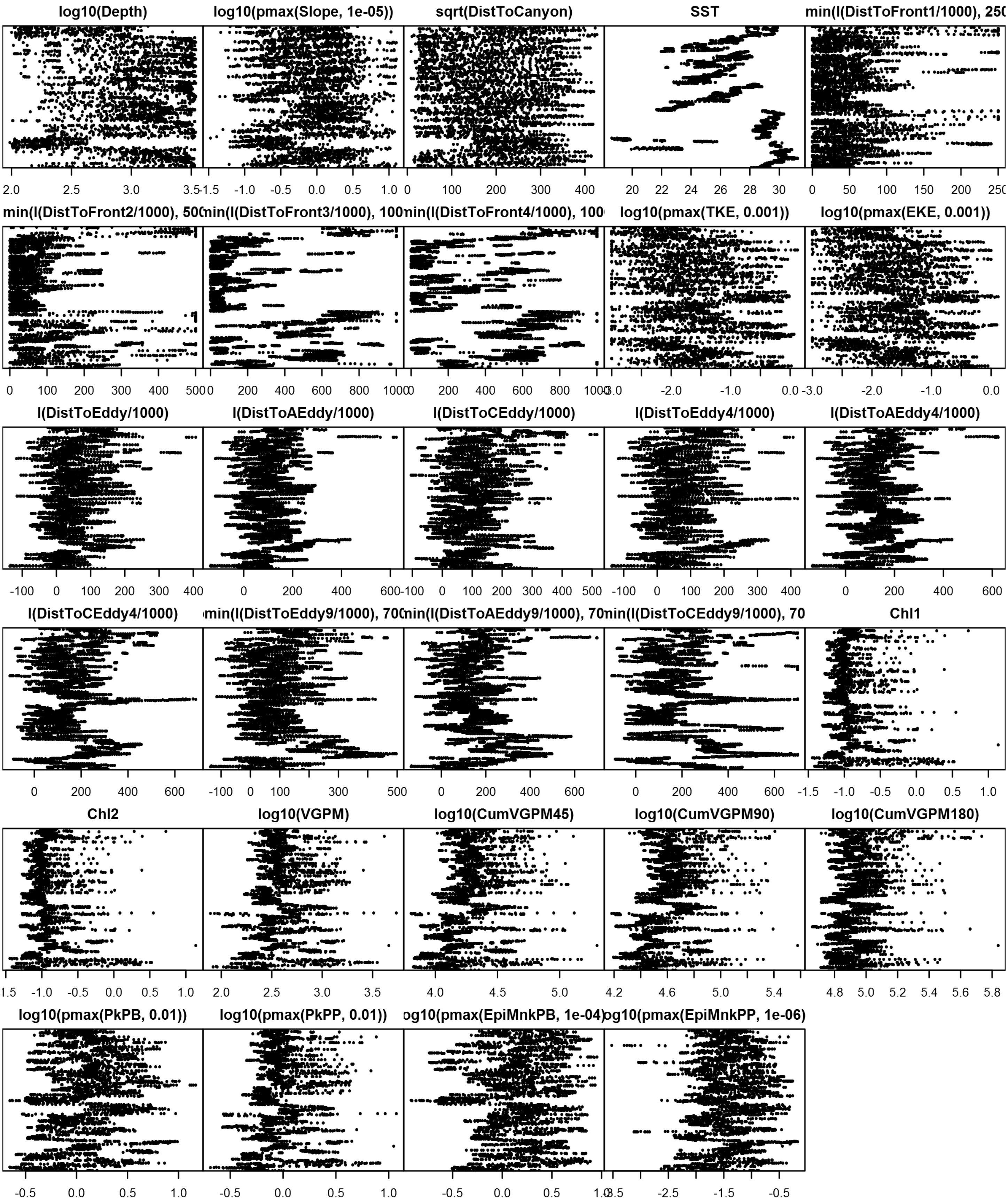

Figure 32: Dotplot for the Beaked whales Contemporaneous model, Off Shelf. This plot is used to check for suspicious patterns and outliers in the data. Points are ordered vertically by transect ID, sequentially in time.

On Shelf

Density assumed to be 0 in this region.

Climatological Same Segments Model

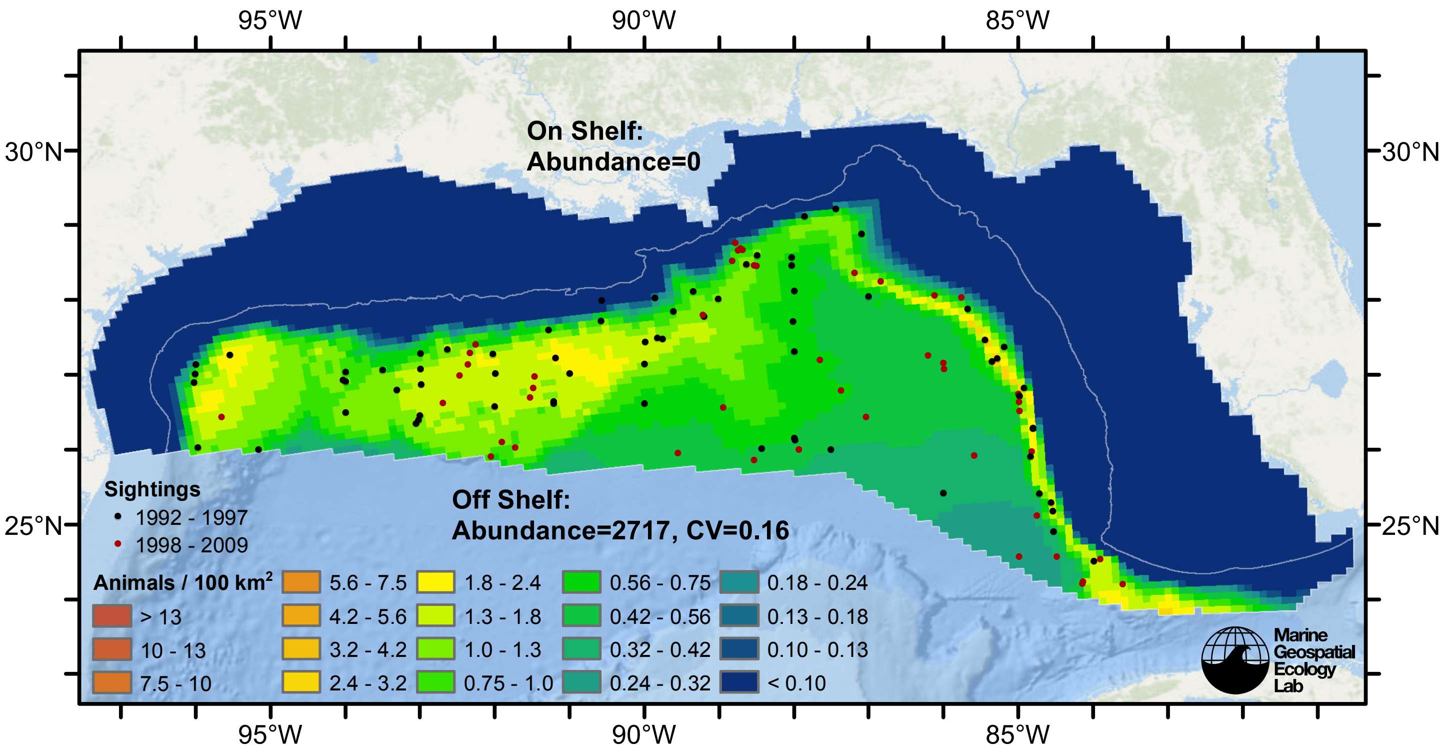

Figure 33: Beaked whales density predicted by the climatological same segments model that explained the most deviance. Pixels are 10x10 km. The legend gives the estimated individuals per pixel; breaks are logarithmic. Abundance for each region was computed by summing the density cells occuring in that region.

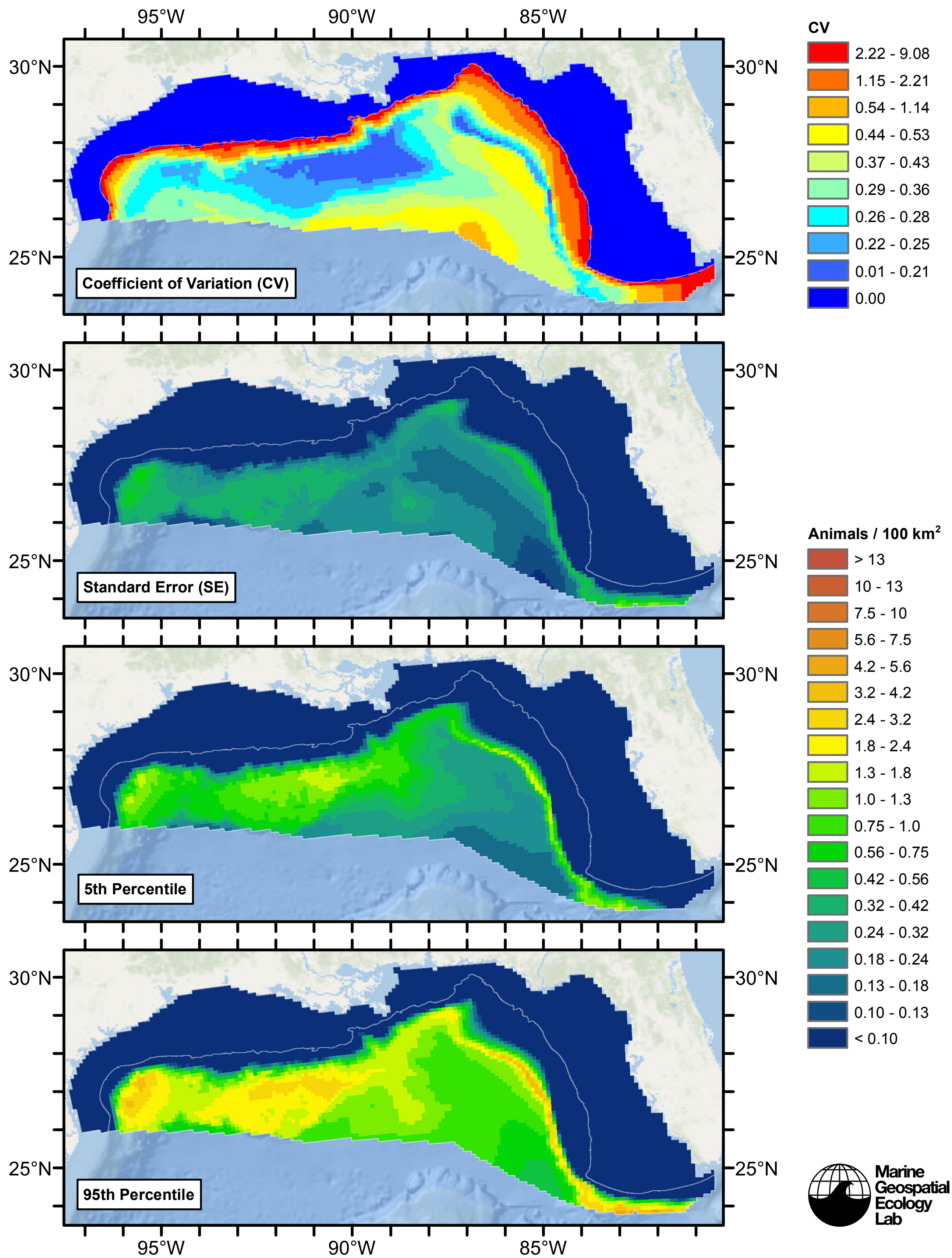

Figure 34: Estimated uncertainty for the climatological same segments model that explained the most deviance. These estimates only incorporate the statistical uncertainty estimated for the spatial model (by the R mgcv package). They do not incorporate uncertainty in the detection functions, g(0) estimates, predictor variables, and so on.

Off Shelf

Statistical output

```
Rscript.exe: This is mgcv 1.8-3. For overview type 'help("mgcv-package")'.


Family: Tweedie(p=1.35)
Link function: log

Formula:
abundance ~ offset(log(area_km2)) + s(log10(Depth), bs = "ts",
    k = 5) + s(pmin(I(ClimDistToFront2/1000), 500), bs = "ts",
    k = 5) + s(I(ClimDistToAEddy/1000), bs = "ts", k = 5) + s(I(ClimDistToCEddy/1000),
    bs = "ts", k = 5)

Parametric coefficients:
            Estimate Std. Error t value Pr(>|t|)
(Intercept)  -7.2965     0.4757  -15.34   <2e-16 ***
---
Signif. codes:  0 '***' 0.001 '**' 0.01 '*' 0.05 '.' 0.1 ' ' 1

Approximate significance of smooth terms:
                                        edf Ref.df      F  p-value
s(log10(Depth))                       2.872      4 11.873 1.38e-11 ***
s(pmin(I(ClimDistToFront2/1000), 500)) 3.683      4  8.621 1.63e-07 ***
s(I(ClimDistToAEddy/1000))            1.837      4  6.322 3.49e-07 ***
s(I(ClimDistToCEddy/1000))            2.380      4  3.992 0.000183 ***
---
Signif. codes:  0 '***' 0.001 '**' 0.01 '*' 0.05 '.' 0.1 ' ' 1

R-sq.(adj) =  -0.00392   Deviance explained = 21.4%
-REML = 1009.6  Scale est. = 72.752    n = 12354

All predictors were significant. This is the final model.
Creating term plots.
Diagnostic output from gam.check():

Method: REML   Optimizer: outer newton
full convergence after 11 iterations.
Gradient range [-4.949603e-07,3.448481e-07]
(score 1009.572 & scale 72.75184).
Hessian positive definite, eigenvalue range [0.2759387,367.9632].
Model rank =  17 / 17

Basis dimension (k) checking results. Low p-value (k-index<1) may
indicate that k is too low, especially if edf is close to k'.

                                         k'   edf k-index p-value
s(log10(Depth))                       4.000 2.872   0.689    0.00
s(pmin(I(ClimDistToFront2/1000), 500)) 4.000 3.683   0.750    0.08
s(I(ClimDistToAEddy/1000))            4.000 1.837   0.745    0.04
s(I(ClimDistToCEddy/1000))            4.000 2.380   0.713    0.00

Predictors retained during the model selection procedure: Depth, ClimDistToFront2, ClimDistToAEddy,
ClimDistToCEddy

Predictors dropped during the model selection procedure: Slope, DistToCanyon, ClimSST, ClimTKE
```

Model term plots

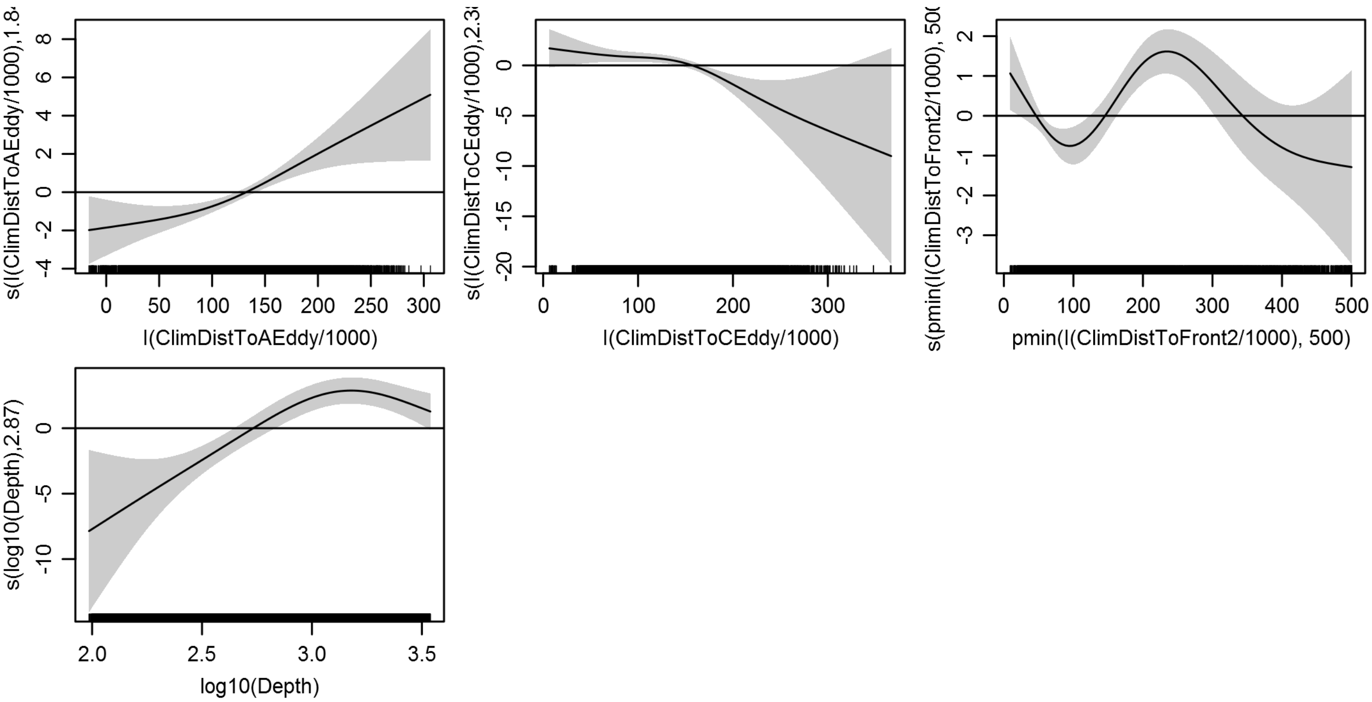

Diagnostic plots

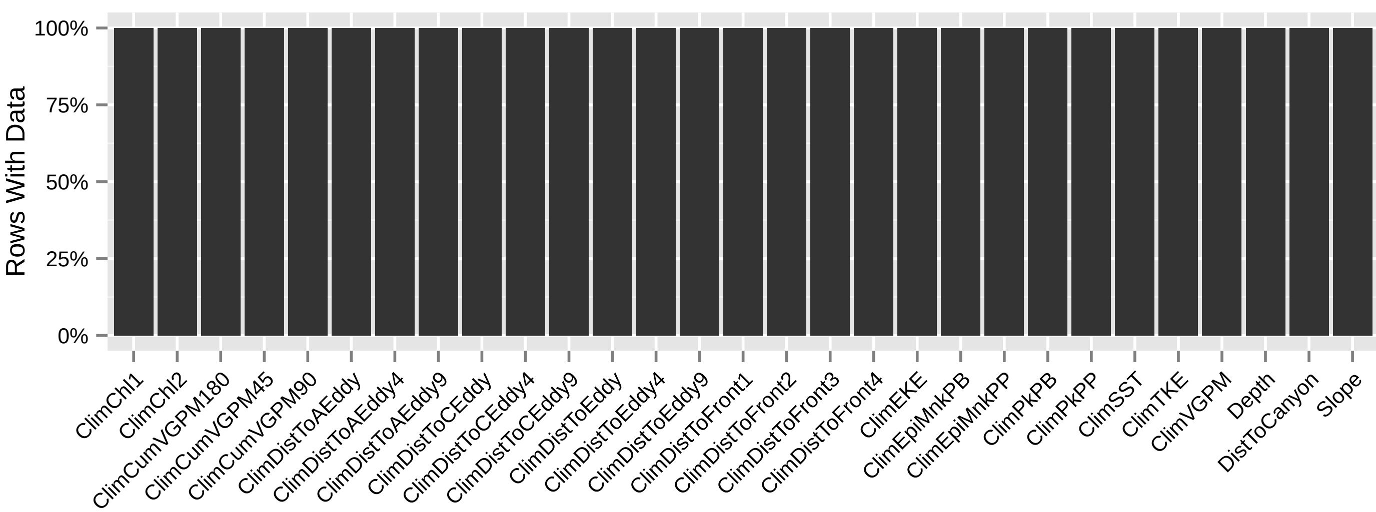

Figure 35: Segments with predictor values for the Beaked whales Climatological model, Off Shelf. This plot is used to assess how many segments would be lost by including a given predictor in a model.

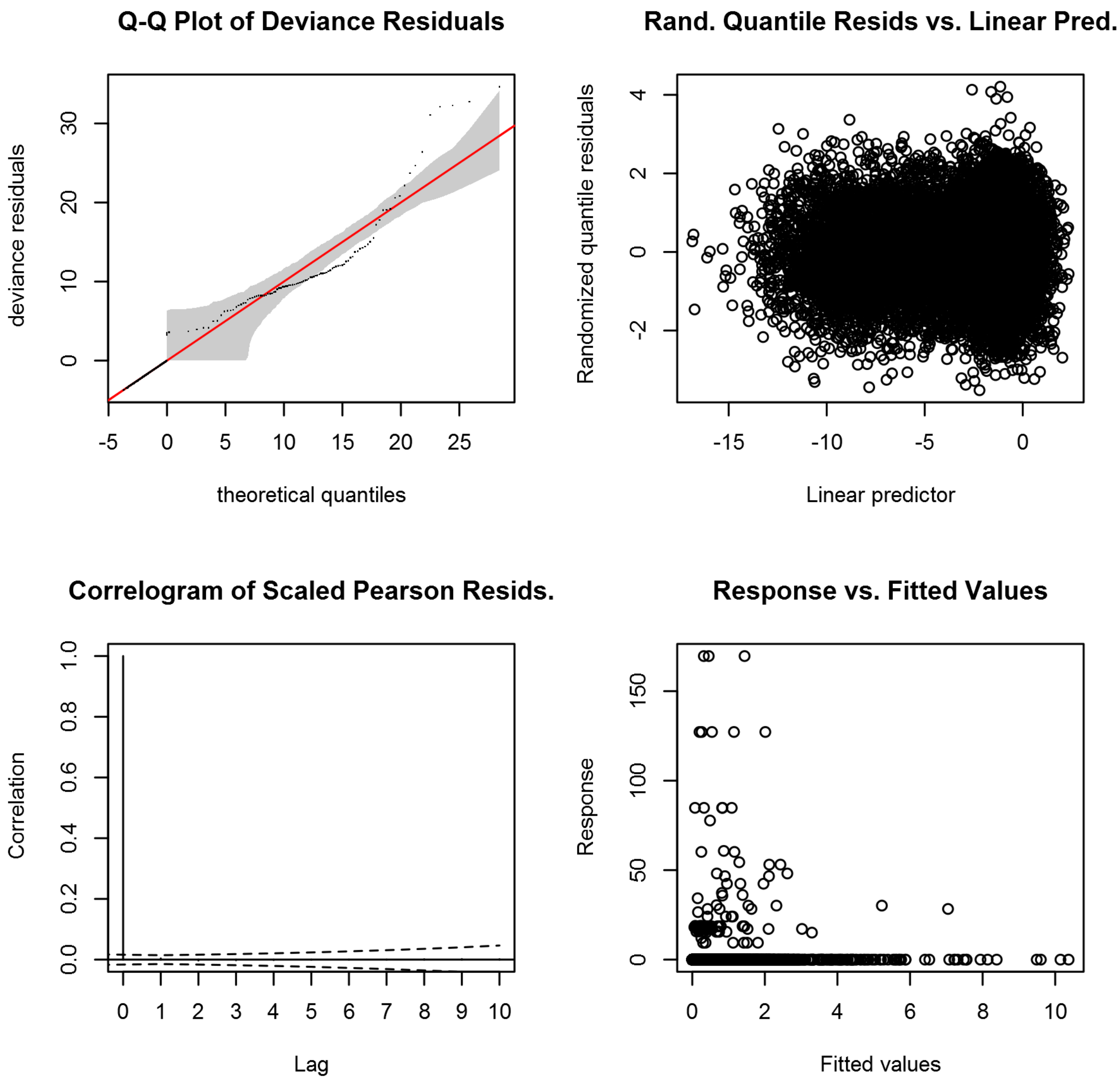

Figure 36: Statistical diagnostic plots for the Beaked whales Climatological model, Off Shelf.

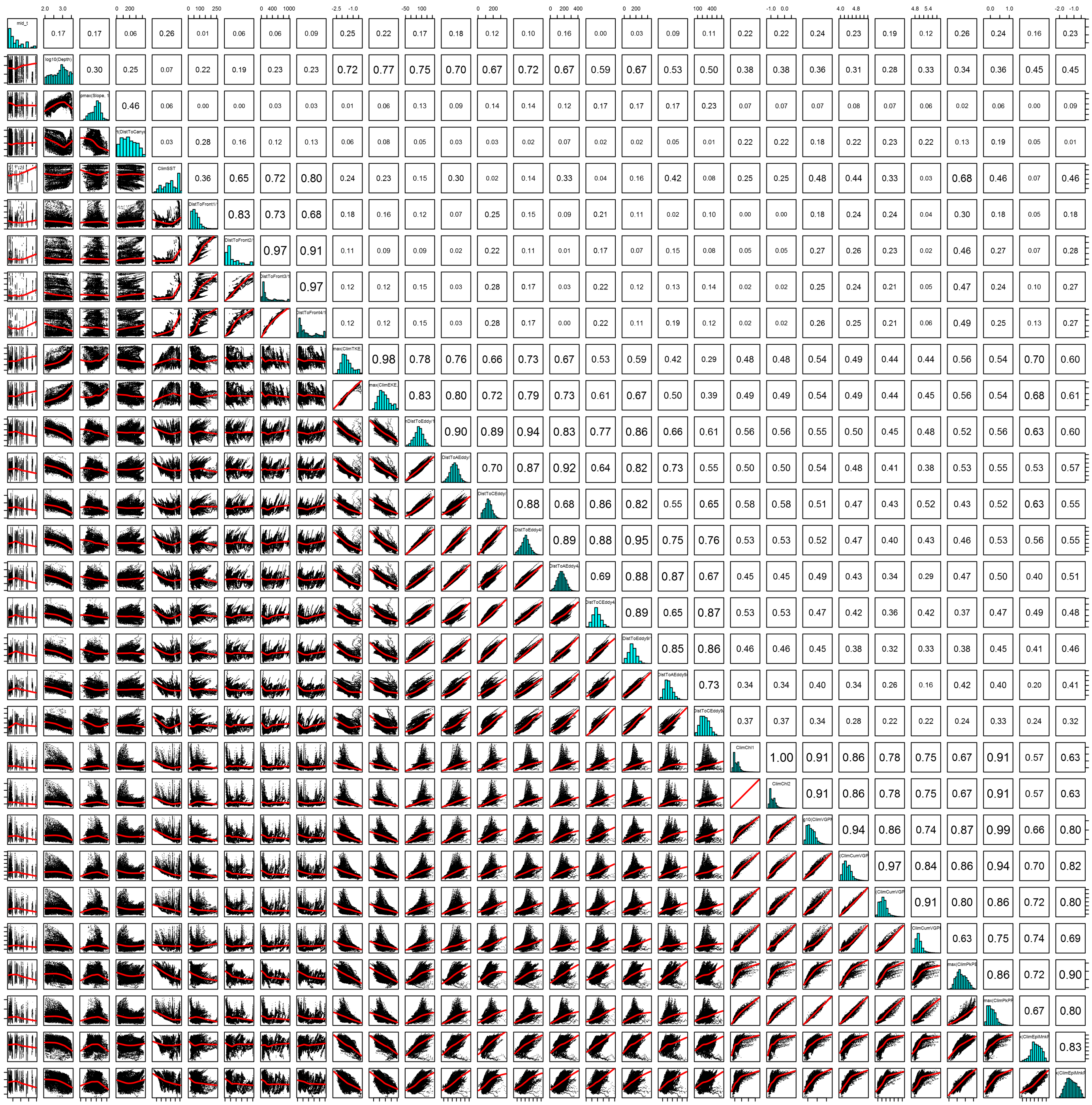

Figure 37: Scatterplot matrix for the Beaked whales Climatological model, Off Shelf. This plot is used to inspect the distribution of predictors (via histograms along the diagonal), simple correlation between predictors (via pairwise Pearson coefficients above the diagonal), and linearity of predictor correlations (via scatterplots below the diagonal). This plot is best viewed at high magnification.

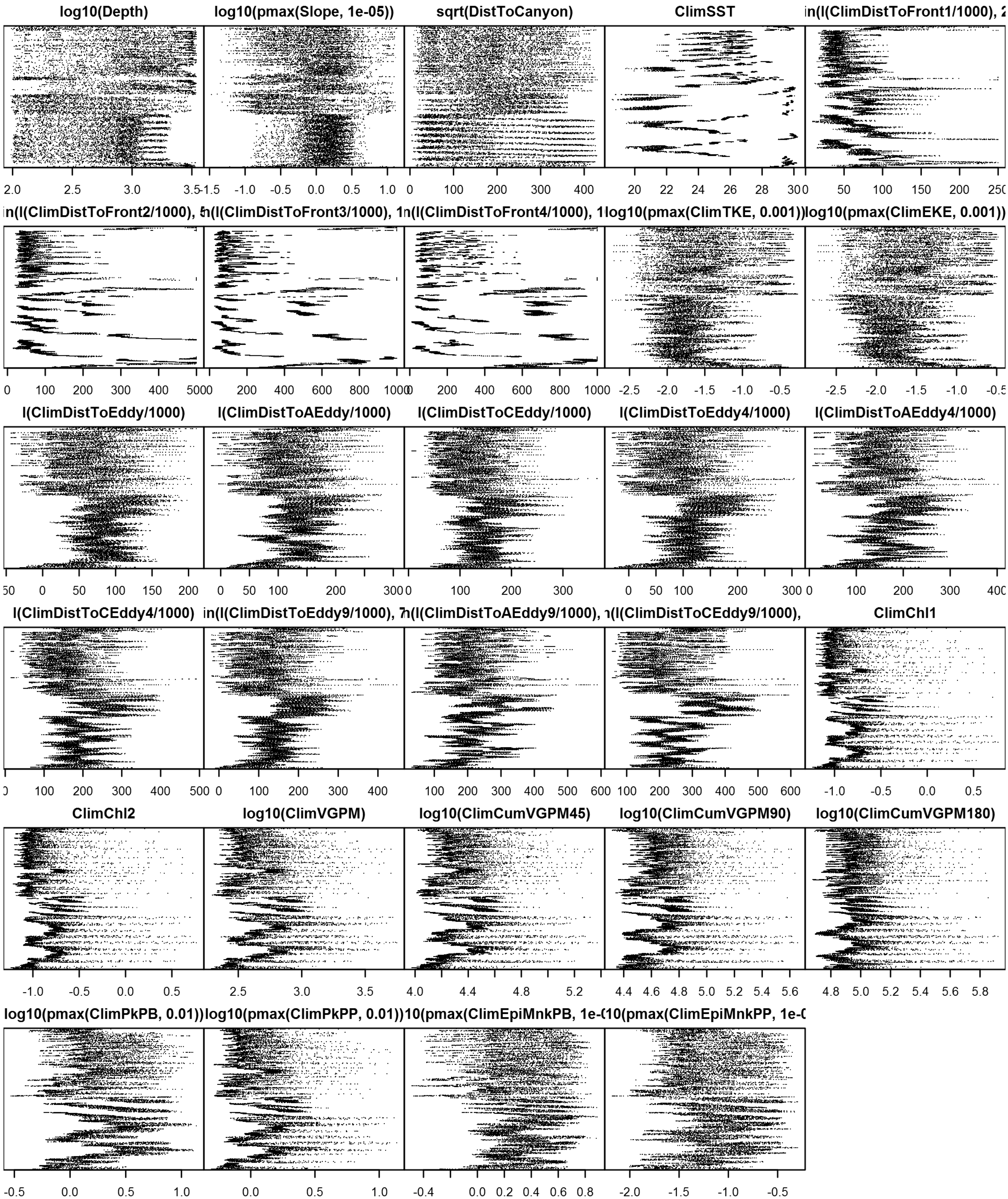

Figure 38: Dotplot for the Beaked whales Climatological model, Off Shelf. This plot is used to check for suspicious patterns and outliers in the data. Points are ordered vertically by transect ID, sequentially in time.

On Shelf

Density assumed to be 0 in this region.

Model Comparison

Spatial Model Performance

The table below summarizes the performance of the candidate spatial models that were tested. The first model contained only physiographic predictors. Subsequent models added additional suites of predictors of based on when they became available via remote sensing.

For each model, three versions were fitted; the % Dev Expl columns give the % deviance explained by each one. The "climatological" models were fitted to 8-day climatologies of the environmental predictors. Because the environmental predictors were always available, no segments were lost, allowing these models to consider the maximal amount of survey data. The "contemporaneous" models were fitted to day-of-sighting images of the environmental predictors; these were smoothed to reduce data loss due to clouds, but some segments still failed to retrieve environmental values and were lost. Finally, the "climatological same segments" models fitted climatological predictors to the segments retained by the contemporaneous model, so that the explantory power of the two types of predictors could be directly compared. For each of the three models, predictors were selected independently via shrinkage smoothers; thus the three models did not necessarily utilize the same predictors.

Predictors derived from ocean currents first became available in January 1993 after the launch of the TOPEX/Poseidon satellite; productivity predictors first became available in September 1997 after the launch of the SeaWiFS sensor. Contemporaneous and climatological same segments models considering these predictors usually suffered data loss. Date Range shows the years spanned by the retained segments. The Segments column gives the number of segments retained; % Lost gives the percentage lost.

Predictors	Climatol % Dev Expl	Contemp % Dev Expl	Climatol Same Segs % Dev Expl	Segments	% Lost	Date Range
Phys	11.3			14455		1992-2009
Phys+SST	9.2	9.2	9.2	14455	0.0	1992-2009
Phys+SST+Curr	16.4	10.3	21.4	12354	14.5	1993-2009
Phys+SST+Curr+Prod	16.2	10.3	21.4	12354	14.5	1993-2009

Table 11: Deviance explained by the candidate density models.

Abundance Estimates

The table below shows the estimated mean abundance (number of animals) within the study area, for the models that explained the most deviance for each model type. Mean abundance was calculated by first predicting density maps for a series of time steps, then computing the abundance for each map, and then averaging the abundances. For the climatological models, we used 8-day climatologies, resulting in 46 abundance maps. For the contemporaneous models, we used daily images, resulting in 365 predicted abundance maps per year that the prediction spanned. The Dates column gives the dates to which the estimates apply. For our models, these are the years for which both survey data and remote sensing data were available.

The Assumed g(0)=1 column specifies whether the abundance estimate assumed that detection was certain along the survey trackline. Studies that assumed this did not correct for availability or perception bias, and therefore underestimated abundance. The In our models column specifies whether the survey data from the study was also used in our models. If not, the study provides a completely independent estimate of abundance.

Dates	Model or study	Estimated abundance	CV	Assumed g(0)=1	In our models

1992-2009	Climatological model*	2910	0.16	No	
1993-2009	Contemporaneous model	2534	0.13	No	
1992-2009	Climatological same segments model	2717	0.16	No	
2009	Ziphius cavirostris, oceanic waters, Jun-Aug (Waring et al. 2013)	74	1.04	Yes	Yes
2009	Mesoplodon spp.	149	0.91	Yes	Yes
2009	Unidentified ziphiid	74	1.04	Yes	Yes
2009	Total, all Ziphiidae	297		Yes	Yes
2003-2004	Ziphius cavirostris, oceanic waters, Jun-Aug (Mullin 2007)	65	0.67	Yes	Yes
2003-2004	Mesoplodon spp.	57	1.40	Yes	Yes
2003-2004	Unidentified ziphiid	337	0.40	Yes	Yes
2003-2004	Total, all Ziphiidae	459		Yes	Yes
1996-2001	Ziphius cavirostris, oceanic waters, Apr-Jun (Mullin and Fulling 2004)	95	0.47	Yes	Yes
1996-2001	Mesoplodon spp.	106	0.41	Yes	Yes
1996-2001	Unidentified ziphiid	146	0.46	Yes	Yes
1996-2001	Total, all Ziphiidae	347		Yes	Yes

Table 12: Estimated mean abundance within the study area. We selected the model marked with * as our best estimate of the abundance and distribution of this taxon. For comparison, independent abundance estimates from NOAA technical reports and/or the scientific literature are shown. Please see the Discussion section below for our evaluation of our models compared to the other estimates. Note that our abundance estimates are averaged over the whole year, while the other studies may have estimated abundance for specific months or seasons. Our coefficients of variation (CVs) underestimate the true uncertainty in our estimates, as they only incorporated the uncertainty of the GAM stage of our models. Other sources of uncertainty include the detection functions and g(0) estimates. It was not possible to incorporate these into our CVs without undertaking a computationally-prohibitive bootstrap; we hope to attempt that in a future version of our models.

Density Maps

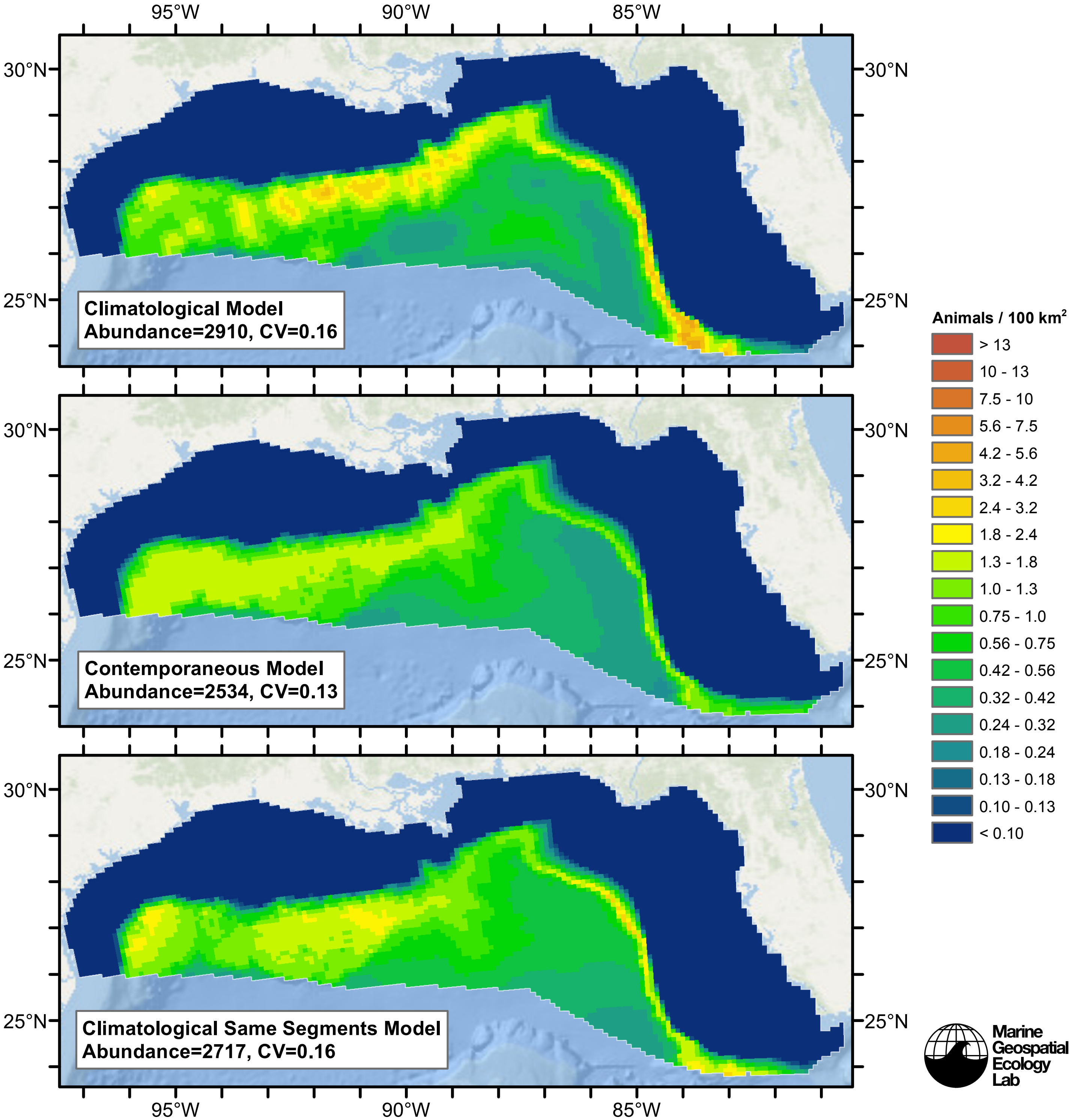

Figure 39: Beaked whales density and abundance predicted by the models that explained the most deviance. Regions inside the study area (white line) where the background map is visible are areas we did not model (see text).

Temporal Variability

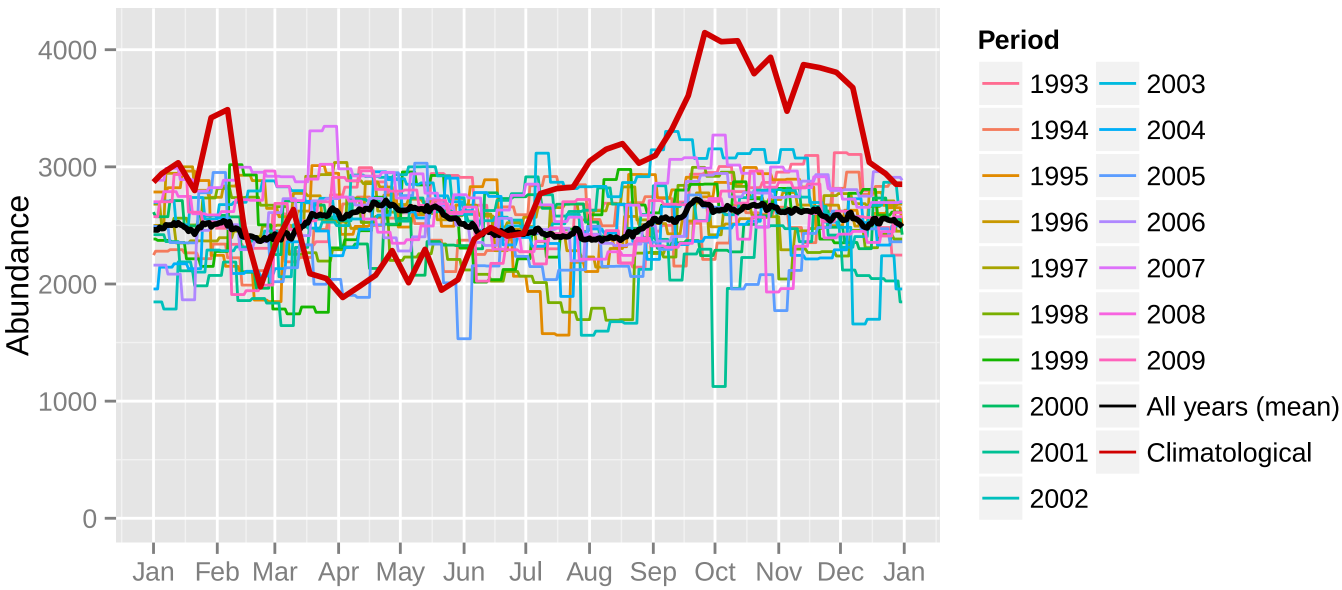

Figure 40: Comparison of Beaked whales abundance predicted at a daily time step for different time periods. Individual years were predicted using contemporaneous models. "All years (mean)" averages the individual years, giving the mean annual abundance of the contemporaneous model. "Climatological" was predicted using the climatological model. The results for the climatological same segments model are not shown.

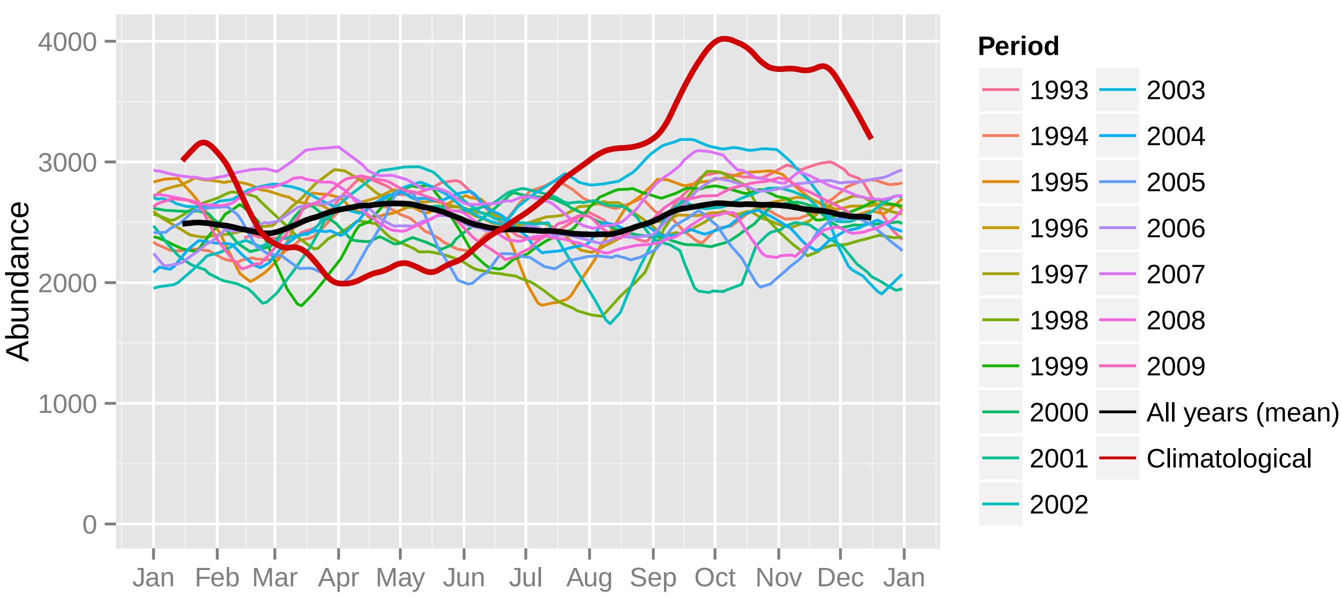

Figure 41: The same data as the preceding figure, but with a 30-day moving average applied.

Climatological Model

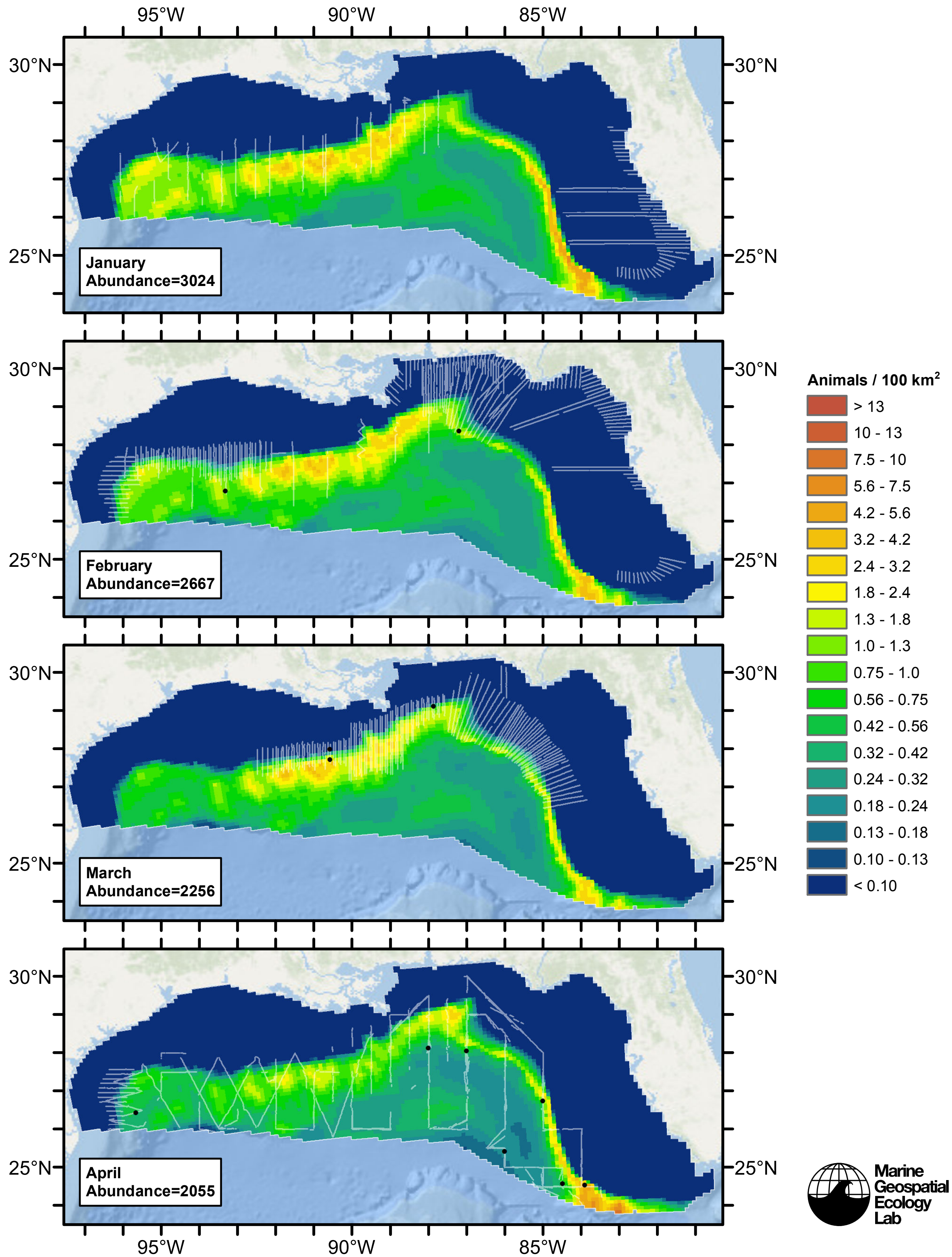

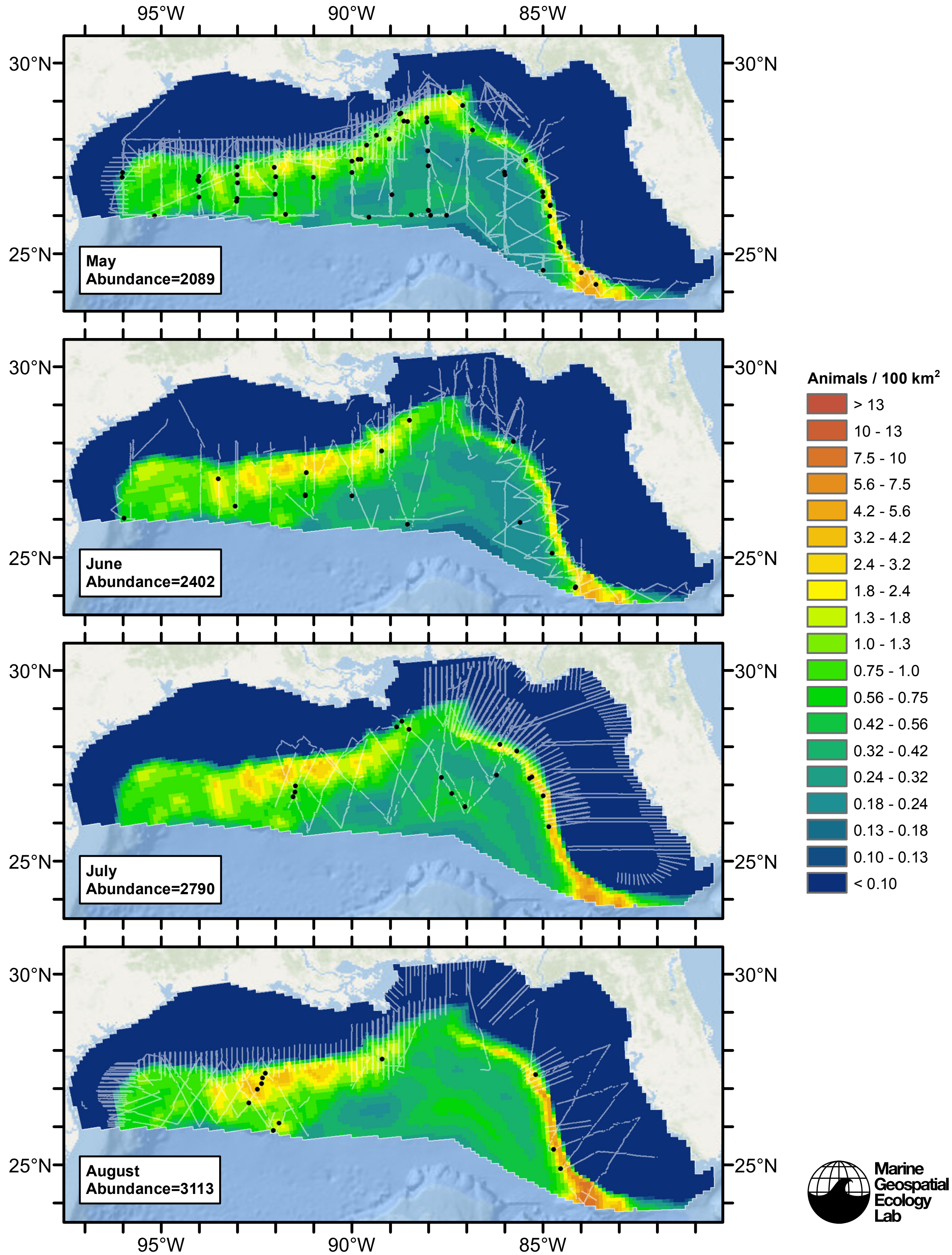
95°W
90°W
85°W
30°N
25°N
May
Abundance=2089
June
Abundance=2402
July
Abundance=2790
August
Abundance=3113
Animals / 100 km²
> 13
10 - 13
7.5 - 10
5.6 - 7.5
4.2 - 5.6
3.2 - 4.2
2.4 - 3.2
1.8 - 2.4
1.3 - 1.8
1.0 - 1.3
0.75 - 1.0
0.56 - 0.75
0.42 - 0.56
0.32 - 0.42
0.24 - 0.32
0.18 - 0.24
0.13 - 0.18
0.10 - 0.13
< 0.10
Marine Geospatial Ecology Lab

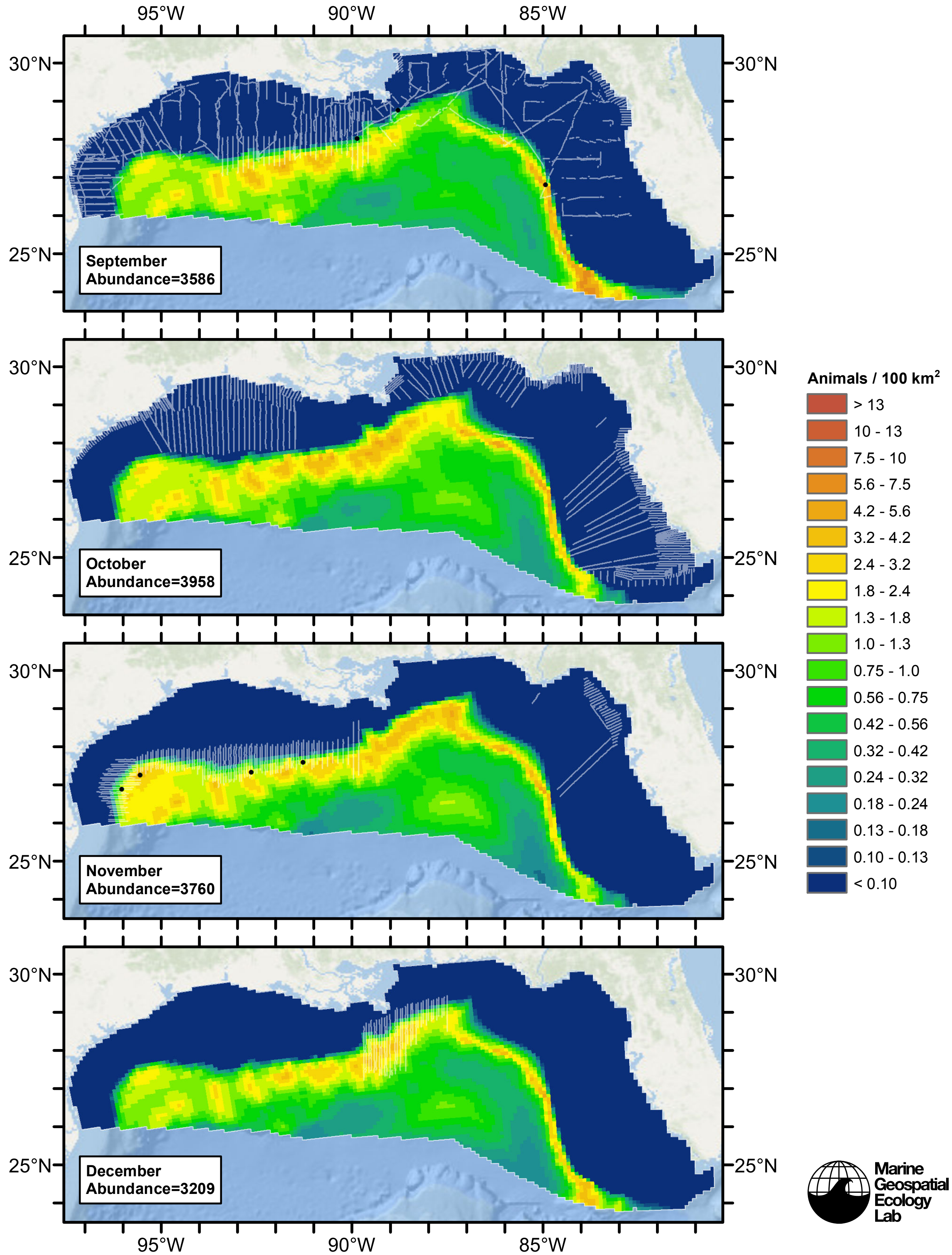
95°W
90°W
85°W
30°N
25°N
September
Abundance=3586
October
Abundance=3958
November
Abundance=3760
December
Abundance=3209
Animals / 100 km²
> 13
10 - 13
7.5 - 10
5.6 - 7.5
4.2 - 5.6
3.2 - 4.2
2.4 - 3.2
1.8 - 2.4
1.3 - 1.8
1.0 - 1.3
0.75 - 1.0
0.56 - 0.75
0.42 - 0.56
0.32 - 0.42
0.24 - 0.32
0.18 - 0.24
0.13 - 0.18
0.10 - 0.13
< 0.10
Marine Geospatial Ecology Lab

Contemporaneous Model

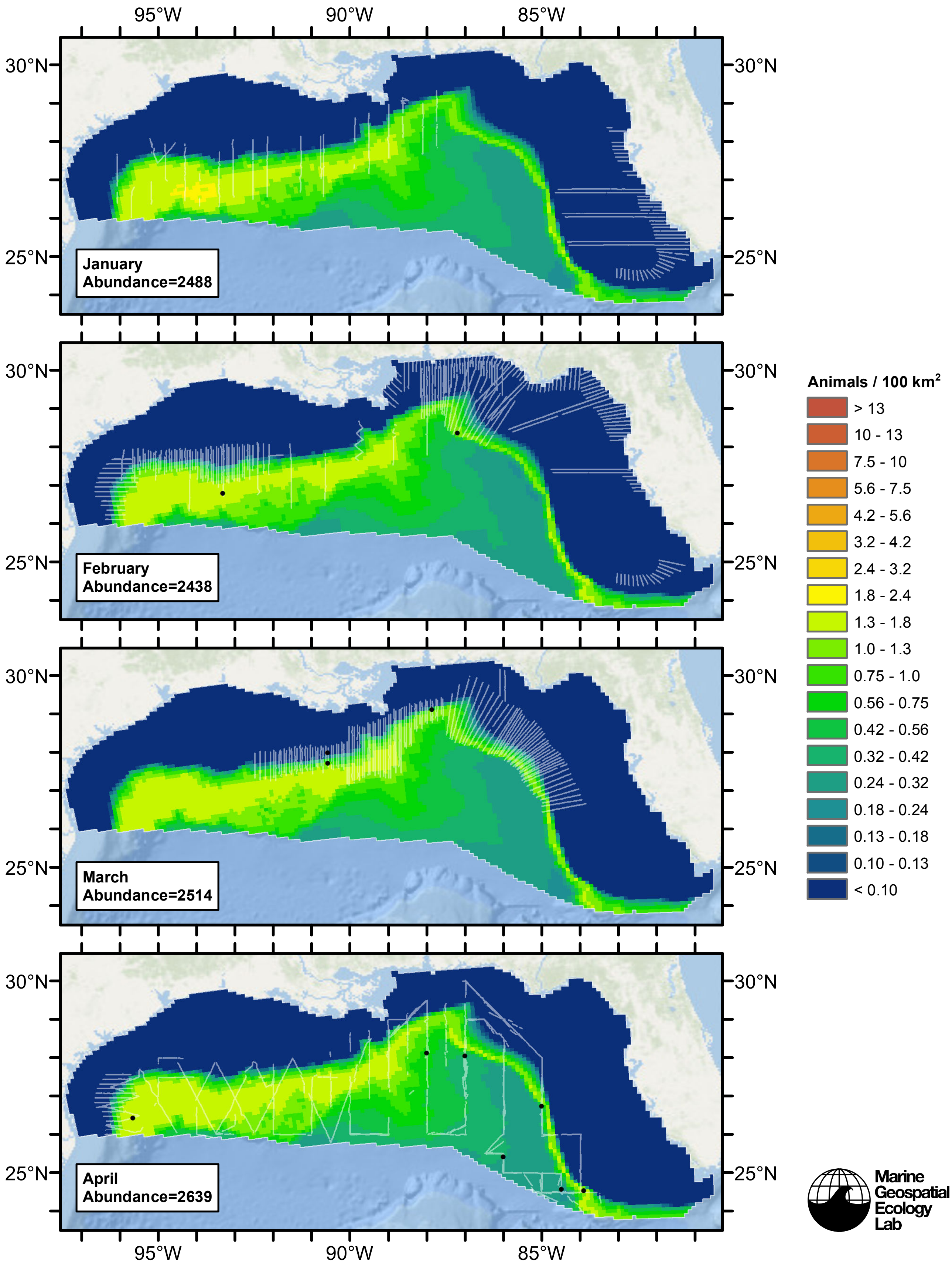

Marine Geospatial Ecology Lab

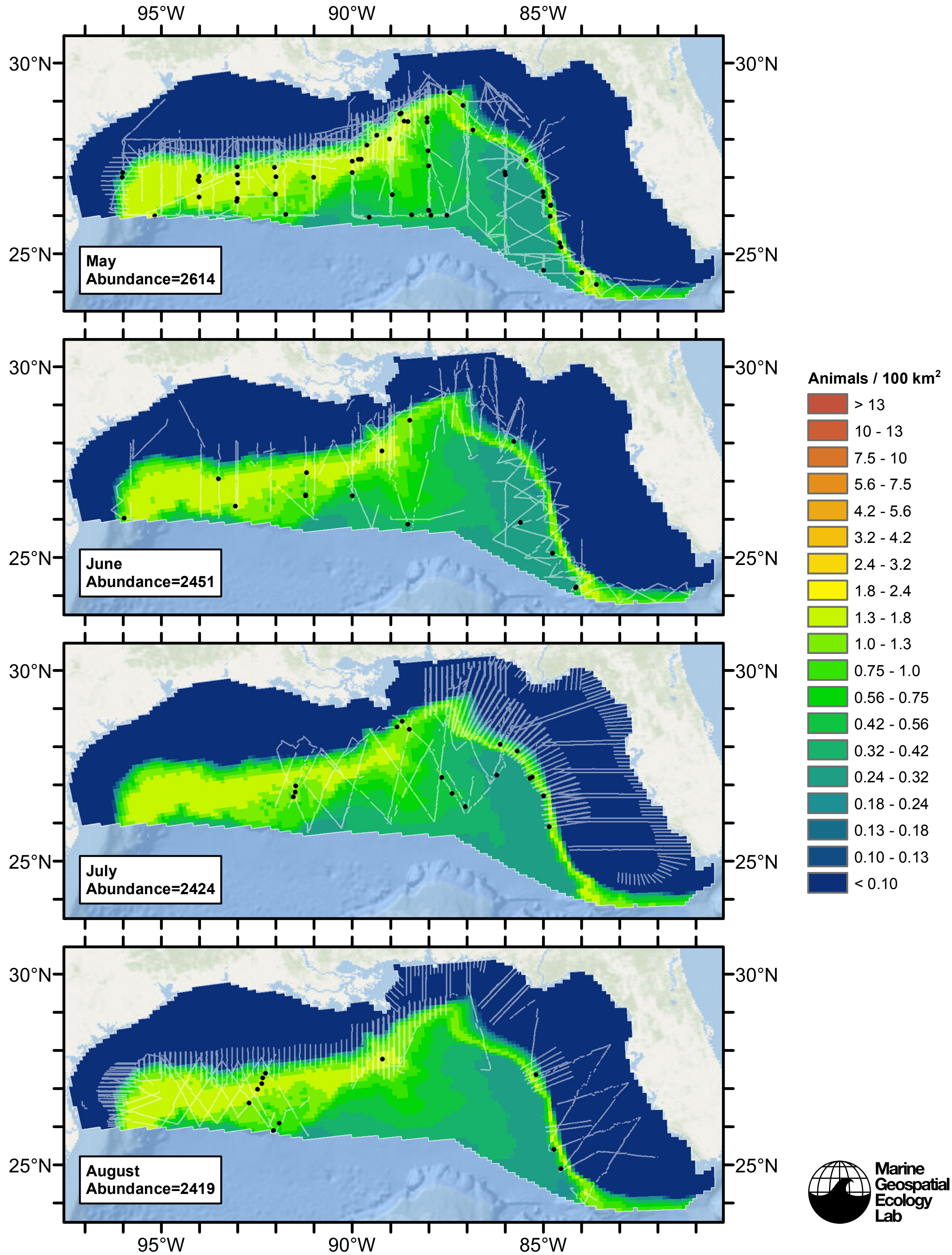
95°W
90°W
85°W
30°N
25°N
May
Abundance=2614
June
Abundance=2451
July
Abundance=2424
August
Abundance=2419
Animals / 100 km²
> 13
10 - 13
7.5 - 10
5.6 - 7.5
4.2 - 5.6
3.2 - 4.2
2.4 - 3.2
1.8 - 2.4
1.3 - 1.8
1.0 - 1.3
0.75 - 1.0
0.56 - 0.75
0.42 - 0.56
0.32 - 0.42
0.24 - 0.32
0.18 - 0.24
0.13 - 0.18
0.10 - 0.13
< 0.10
Marine
Geospatial
Ecology
Lab

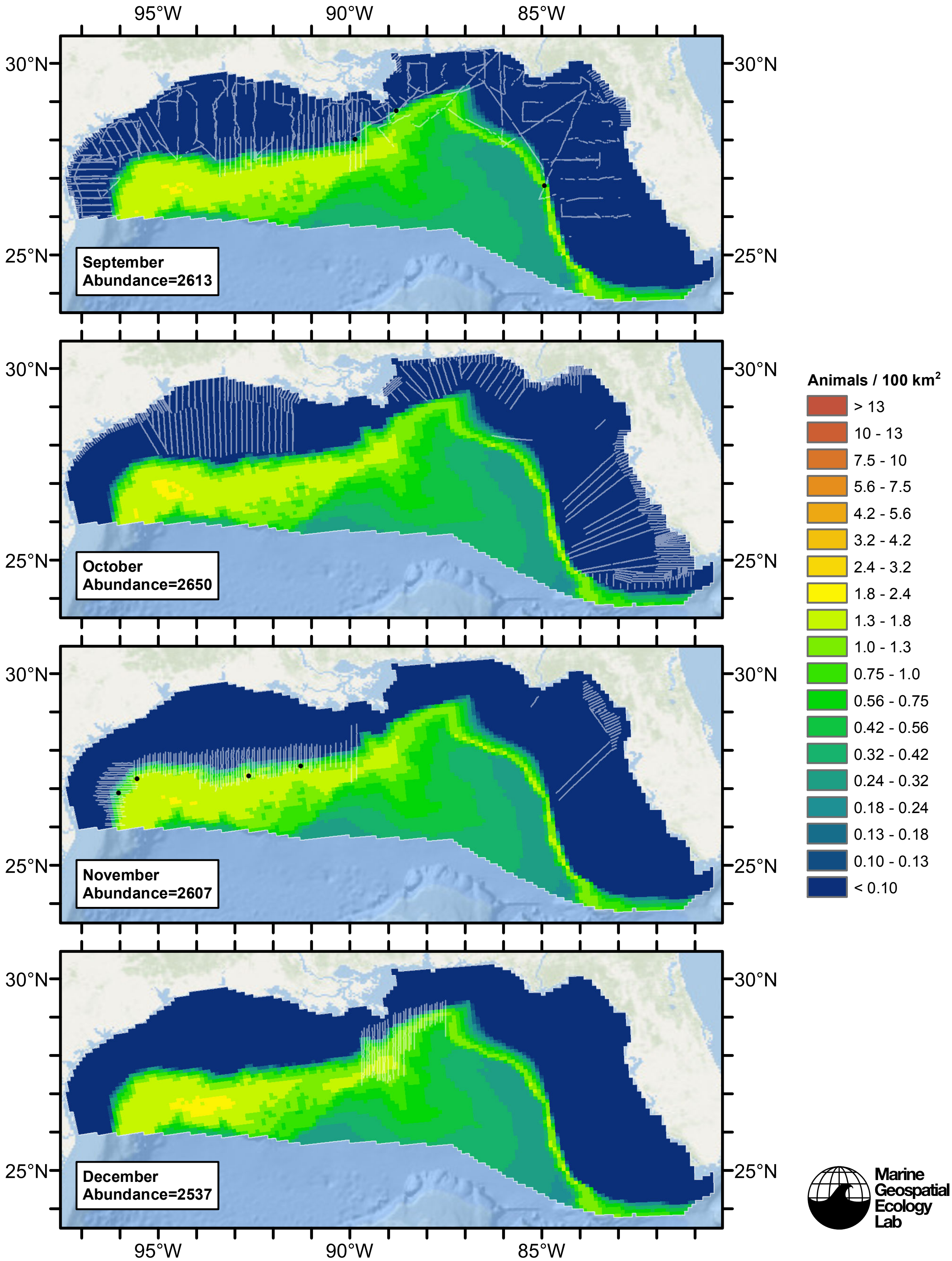

95°W
90°W
85°W
30°N
25°N
September
Abundance=2613
October
Abundance=2650
November
Abundance=2607
December
Abundance=2537
Animals / 100 km²
> 13
10 - 13
7.5 - 10
5.6 - 7.5
4.2 - 5.6
3.2 - 4.2
2.4 - 3.2
1.8 - 2.4
1.3 - 1.8
1.0 - 1.3
0.75 - 1.0
0.56 - 0.75
0.42 - 0.56
0.32 - 0.42
0.24 - 0.32
0.18 - 0.24
0.13 - 0.18
0.10 - 0.13
< 0.10
Marine Geospatial Ecology Lab

Climatological Same Segments Model

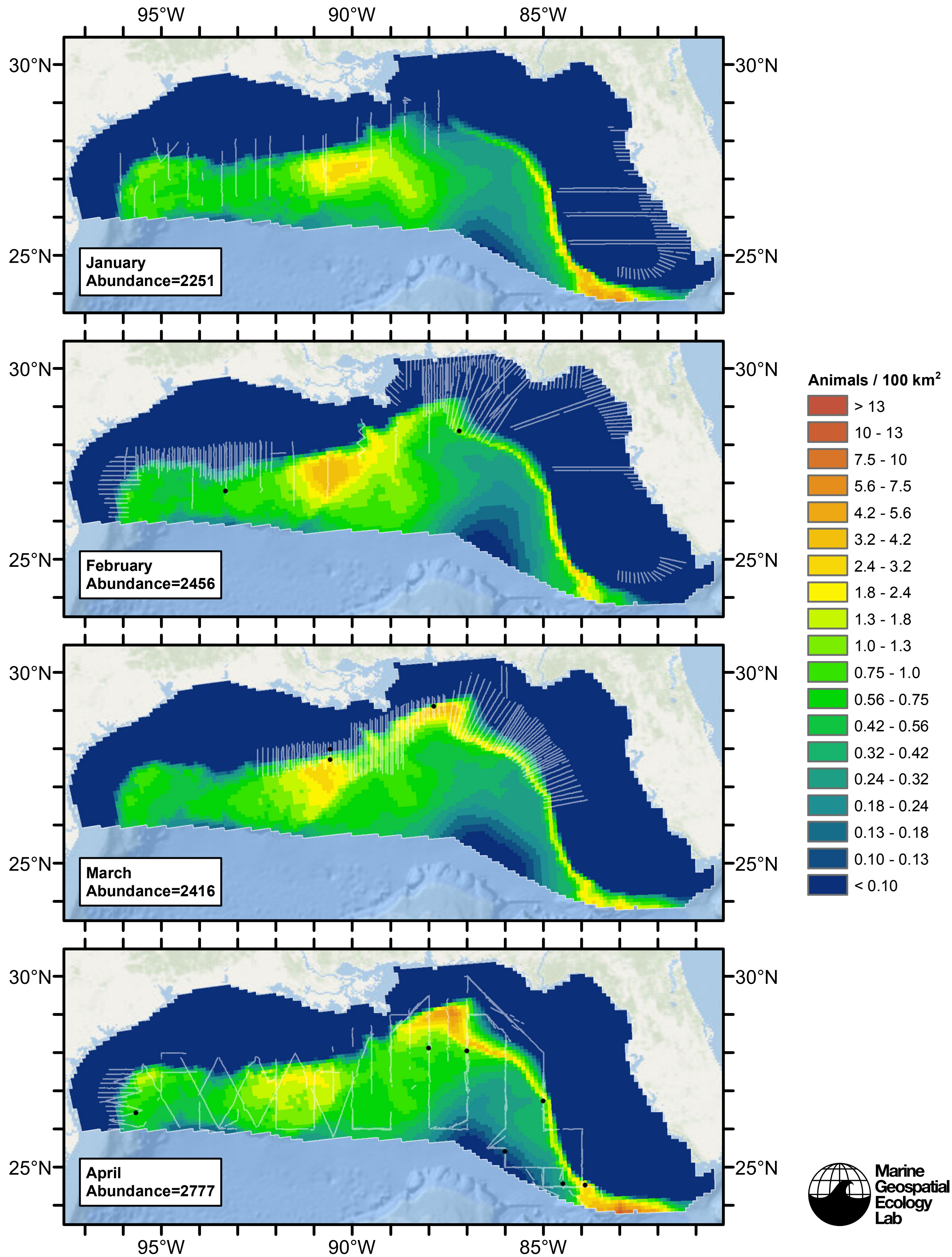

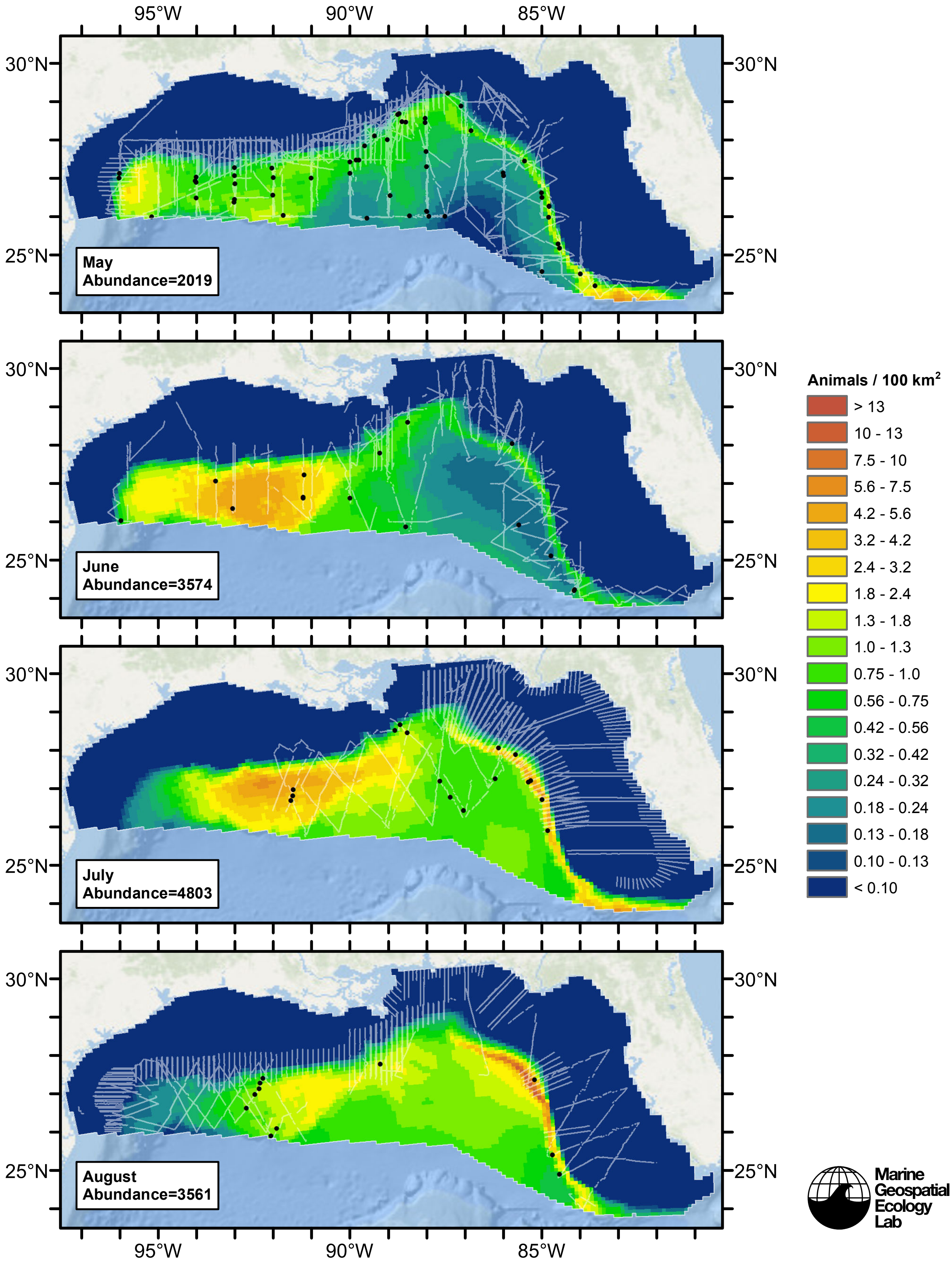

Marine Geospatial Ecology Lab

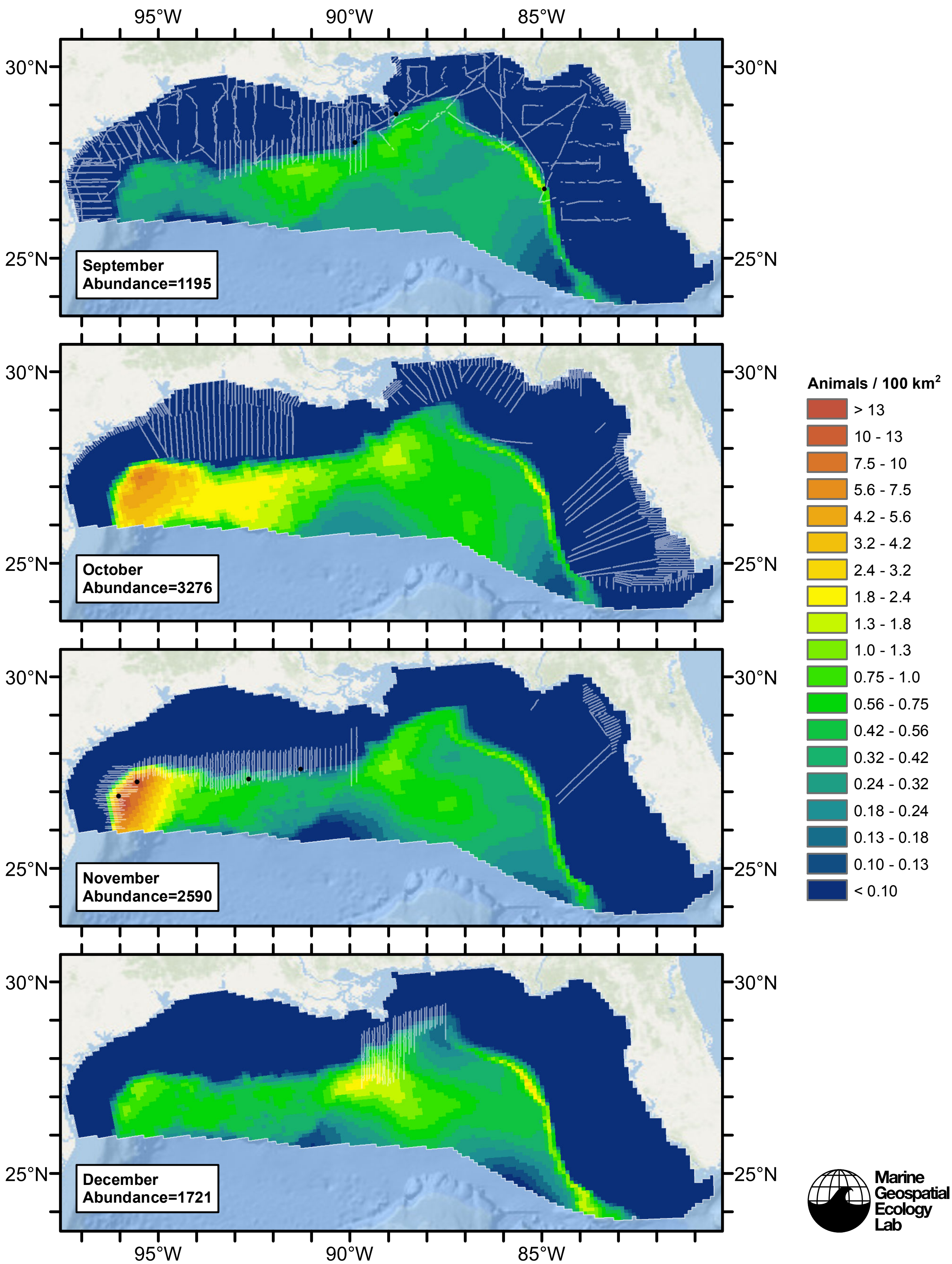
95°W
90°W
85°W
30°N
25°N
September
Abundance=1195
October
Abundance=3276
November
Abundance=2590
December
Abundance=1721
Animals / 100 km²
> 13
10 - 13
7.5 - 10
5.6 - 7.5
4.2 - 5.6
3.2 - 4.2
2.4 - 3.2
1.8 - 2.4
1.3 - 1.8
1.0 - 1.3
0.75 - 1.0
0.56 - 0.75
0.42 - 0.56
0.32 - 0.42
0.24 - 0.32
0.18 - 0.24
0.13 - 0.18
0.10 - 0.13
< 0.10
Marine
Geospatial
Ecology
Lab

Discussion

Models built with climatological predictors explained substantially more deviance than models built with contemporaneous predictors. On this basis, we selected the climatological predictor model fitted to all segments as our as our best estimate of beaked whale density and abundance.

The higher explanatory power in climatological predictors contrasted with our beaked whale models for the east coast study area, where the contemporaneous predictors provided more explanatory power. But the models in the two regions utilized similar covariates, including depth, distance to canyons, distance to eddies, and cumulative primary productivity over the last 90 days, suggesting that beaked whale density is related to similar environmental processes in both areas. In the Gulf of Mexico, our selected model predicted high density along the continental slope, near canyons, cyclonic eddies, and areas of high primary productivity, and away from anticyclonic eddies.

Because the survey effort used as input to this model was biased toward spring and summer and was spatiotemporally patchy (see maps in the Temporal Variability section above), we were not confident that our models could produce realistic predictions at a monthly temporal resolution. This problem affected all species that we modeled in the Gulf of Mexico, and we recommend that year-round average predictions be used for all Gulf of Mexico species.

NOAA's abundance estimates for all Ziphiidae were somewhat variable, at 297 for 2009, 459 for 2003-2004, and 347 for 1996-2001. Our estimate, 2910, exceeded these by an order of magnitude. We believe the biggest factor contributing to this difference concerns the g(0) parameter: NOAA's estimates assumed that g(0)=1 while we applied g(0)=0.23 for shipboard sightings and g(0)=0.074 sightings. As described in the g(0) Estimates section above, beaked whales are long diving animals, leading to high availability bias particularly from aircraft. All else being equal, utilizing our g(0) estimates rather than NOAA's would lead to a 4.3x higher abundance than NOAAs for beaked whales sighted by shipboard observers, and a 13.5x higher abundance for beaked whales sighted by aerial observers. Thus it is not surprising that our estimate would be an order of magnitude higher than NOAA's.

We note that, at the time of this writing, NOAA's most recent abundance estimate of 297 is what NOAA used to estimate stock-level parameters important to management, including the Minimum Population Estimate (Nmin) and the Potential Biological Removal (PBR). Because these estimates are very low relative to the abundance we estimated, it is likely that if our results are used to estimate population-level impacts from potentially harmful human activities (i.e. "takes", as defined by the Marine Mammal Protection Act), the estimated impacts will be very high relative NOAA's estimated stock size (i.e. the estimated takes will greatly exceed PBR).

There is no easy solution to this problem. One possibility is that NOAA could recalculate stock-level parameters such as Nmin and PBR using our results. But this would violate NOAA's guideline that data older than 8 years not be used to estimate stock-level parameters (Moore et al. 2011). Alternatively, impacts could be estimated using NOAA's abundance estimate of 297, computing density by dividing this number by the total area of the off-shelf portion of the U.S. Exclusive Economic Zone in the Gulf of Mexico. But this would fail to account for the non-uniform distribution of beaked whales predicted by our study. Finally, in a hybrid approach, a new density surface could be obtained by apportioning NOAA's abundance estimate of 297 proportionally according to the density surface predicted by our models. To do that, divide our density surface by our total estimated abundance (2910), then multiply every cell by 297. To check that the result computed correctly, sum up all of the cells; the result should equal 297. This new density surface would reflect the distribution pattern predicted by our study but use the total abundance estimate from NOAA.

Interested parties should consult with NOAA about the best way to proceed with this problem.

References

Baird RW, Webster DL, McSweeney DJ, Ligon AD, Schorr GS, Barlow J (2006) Diving behaviour of Cuvier's (Ziphius cavirostris) and Blainville's (Mesoplodon densirostris) beaked whales in Hawai'i. Can J Zool 84: 1120-1128.

Barlow J (1999) Trackline detection probability for long diving whales. In: Marine Mammal Survey and Assessment Methods (Garner GW, Amstrup SC, Laake JL, Manly BFJ, McDonald LL, Robertson DG, eds.). Balkema, Rotterdam, pp. 209-221.

Barlow J, Oliver CW, Jackson TD, Taylor BL (1988) Harbor Porpoise, Phocoena phocoena, Abundance Estimation for California, Oregon, and Washington: II. Aerial Surveys. Fishery Bulletin 86: 433-444.

Carretta JV, Lowry MS, Stinchcomb CE, Lynn MS, Cosgrove RE (2000) Distribution and abundance of marine mammals at San Clemente Island and surrounding offshore waters: results from aerial and ground surveys in 1998 and 1999. Administrative Report LJ-00-02, available from Southwest Fisheries Science Center, P.O. Box 271, La Jolla, CA USA 92038. 44 p.

MacLeod CD, D'Amico A (2006) A review of beaked whale behaviour and ecology in relation to assessing and mitigating impacts of anthropogenic noise. Journal of Cetacean Research and Management 7: 211-221.

Madsen PT, Aguilar de Soto N, Tyack PL, Johnson M (2014) Beaked whales. Current Biology 24: R728-R730.

Moore JE, Merrick RL, Angliss R, Barlow J, Bettridge S, Caretta J, et al. (2011) Guidelines for Assessing Marine Mammal Stocks: Report of the GAMMS III Workshop, February 15-18, 2011, La Jolla, California. US Department of Commerce, National Oceanic and Atmospheric Administration, National Marine Fisheries Service, Office of Protected Resources.

Moors-Murphy HB (2014) Submarine canyons as important habitat for cetaceans, with special reference to the Gully: A review. Deep Sea Research Part II: Topical Studies in Oceanography 104: 6-19.

Mullin KD (2007) Abundance of cetaceans in the oceanic Gulf of Mexico based on 2003-2004 ship surveys. 26 pp.

Mullin KD, Fulling GL (2004) Abundance of cetaceans in the oceanic northern Gulf of Mexico. Mar. Mamm. Sci. 20(4): 787-807.

Schorr GS, Falcone EA, Moretti DJ, Andrews RD (2014) First Long-Term Behavioral Records from Cuvier's Beaked Whales (Ziphius cavirostris) Reveal Record-Breaking Dives. PLoS ONE. 9: e92633.

Tyack PL, Johnson M, Soto NA, Sturlese A, Madsen PT (2006) Extreme diving of beaked whales. Journal of Experimental Biology 209: 4238-4253.

Waring GT, Josephson E, Maze-Foley K, Rosel PE, eds. (2013) U.S. Atlantic and Gulf of Mexico Marine Mammal Stock Assessments – 2012. NOAA Tech Memo NMFS NE 223; 419 p.

Waring GT, Josephson E, Maze-Foley K, Rosel PE, eds. (2014) U.S. Atlantic and Gulf of Mexico Marine Mammal Stock Assessments – 2013. NOAA Tech Memo NMFS NE 228; 464 p.